

AD-A108 095

ARIZONA UNIV TUCSON ENGINEERING EXPERIMENT STATION
CONVECTIVE HEAT TRANSFER FOR SHIP PROPULSION.(U)

F/G 20/13

APR 81 M A HABIB, D W MCELIGOT
1246-8

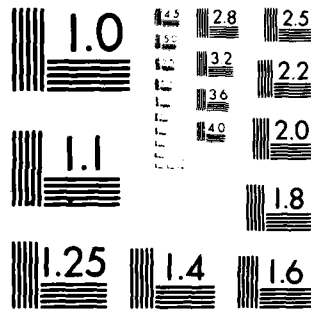
N00014-75-C-0694

NL

UNCLASSIFIED

2
A-000000

0 0



MICROCOPY RESOLUTION TEST CHART
NATIONAL BUREAU OF STANDARDS-1963-A

30
AD A108095

12

10

Sixth Annual Summary Report

Contract No. N00014-75-C-0694
Contract Authority NR-097-395

LEVEL

CONVECTIVE HEAT TRANSFER FOR SHIP PROPULSION

Prepared for

Office of Naval Research
Code 473
Arlington, Virginia

Prepared by

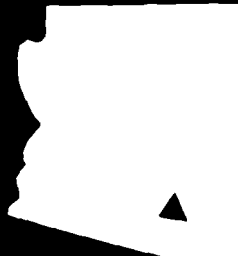
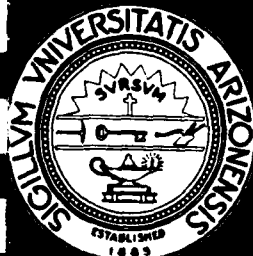
M. A. Habib and D. M. McEligot

1 April 1981

DISTRIBUTION STATEMENT A

Approved for public release;
Distribution Unlimited

DTIC
ELECTE
S DEC 3 1981 D
D



DTIC FILE COPY

**ENGINEERING EXPERIMENT STATION
COLLEGE OF ENGINEERING
THE UNIVERSITY OF ARIZONA
TUCSON, ARIZONA 85721**

REPORT DOCUMENTATION PAGE		READ INSTRUCTIONS BEFORE COMPLETING FORM
1. REPORT NUMBER 1248-8	2. GOVT ACCESSION NO. AD-A108095	3. RECIPIENT'S CATALOG NUMBER
4. TITLE (and Subtitle) Convective Heat Transfer for Ship Propulsion. (Sixth Annual Summary Report)		5. TYPE OF REPORT & PERIOD COVERED Annual Summary Report. 15 Jan 1980-30 March 1981
7. AUTHOR(s) M. A. Habib and D. M. McEligot		6. PERFORMING ORG. REPORT NUMBER
9. PERFORMING ORGANIZATION NAME AND ADDRESS Engineering Experiment Station University of Arizona Tucson, Arizona 85721		8. CONTRACT OR GRANT NUMBER(s) N00014-75-C-0694
11. CONTROLLING OFFICE NAME AND ADDRESS Office of Naval Research Code 473 Arlington, Virginia 22217		10. PROGRAM ELEMENT, PROJECT, TASK AREA & WORK UNIT NUMBERS NR-097-395
14. MONITORING AGENCY NAME & ADDRESS (if different from Controlling Office) Office of Naval Research Bandolier Hall West - Rm. 204 University of New Mexico Albuquerque, N. M. 87131		12. REPORT DATE 1 April 1981
		13. NUMBER OF PAGES 100
		15. SECURITY CLASS. (of this report) Unclassified
16. DISTRIBUTION STATEMENT (of this Report) Unlimited		15a. DECLASSIFICATION/DOWNGRADING SCHEDULE
<div style="border: 1px solid black; padding: 5px; text-align: center;">DISTRIBUTION STATEMENT A Approved for public release; Distribution Unlimited</div>		
17. DISTRIBUTION ST.	18. DISTRIBUTION STATEMENT (of abstract entered in Block 20, if different from Report)	
Unlimited		
19. SUPPLEMENTARY NOTES		
19. KEY WORDS (Continue on reverse side if necessary and identify by block number) Heat transfer Turbulence model Turbulent flow Forced convection Swirl Elliptic partial differential equations Sudden expansion Inlets		
20. ABSTRACT (Continue on reverse side if necessary and identify by block number) A common geometry recurring in compact Naval propulsion plants is a change in duct size in the primary fluid loop. As a consequence of the upstream plumbing, the fluid is often swirling about the axis in the piping. Heat losses from the primary fluid and thermal stresses in the component depend on the convective heat transfer from the fluid to the component as it undergoes this geometrical transition. The idealized problem is a study of heat transfer in a sudden expansion with swirl flow, the subject of the present report. The same situation also occurs at the entrance to some heat exchanger tubes.		

Calculations of the flow and heat transfer of a swirling turbulent flow after a sudden pipe expansion are reported. The calculations were obtained by the numerical solution of the time-averaged forms of the continuity, momentum and thermal energy equations together with equations for the turbulence kinetic energy and its rate of dissipation. For a sudden expansion without swirl, the predictions produced satisfactory agreement with available data for the Nusselt number. In the swirling case, there were no heat transfer measurements available for comparison. However, existing measurements of a swirl flow at an expansion without heat transfer were used to test the validity of the flow field calculations.

The predicted effects of varying the swirl number from zero to 1.0 on the heat transfer behavior are presented for a range of Prandtl numbers from 0.7 to 10. The expected effects of the swirl on the velocity and temperature fields are also reported. The results predict, for example, that the maximum Nusselt number is increased as the swirl number increases and its position moves towards the inlet section. They also show an increase in the Nusselt number as the Prandtl number increases.

Unclassified

SECURITY CLASSIFICATION OF THIS PAGE(When Data Entered)

Sixth Annual Summary Report

CONVECTIVE HEAT TRANSFER FOR SHIP PROPULSION

By

M. A. Habib and D. M. McEligot
Aerospace and Mechanical Engineering Department
University of Arizona
Tucson, Arizona 85721

Research Sponsored by

Office of Naval Research
ONR Contract Number N00014-75-C-0694
ONR Contract Authority NR-097-395

Accession For	
NTIS GRA&I	<input checked="checked" type="checkbox"/>
DTIC TAB	<input type="checkbox"/>
Unannounced	<input type="checkbox"/>
Justification	
By _____	
Distribution/	
Availability Codes	
Dist	Avail and/or Special
A	

1 April 1981

DTIC
ELECTE
S DEC 3 1981 D
D

Approved for public release; distribution unlimited. Reproduction in whole or in part is permitted for any purpose of the United States Government.

CONVECTIVE HEAT TRANSFER FOR SHIP PROPULSION

M. A. Habib* and D. M. McEligot
Aerospace and Mechanical Engineering Department
University of Arizona, Tucson, Ariz. 85721 USA

Abstract

Calculations of the flow and heat transfer of a swirling turbulent flow after a sudden pipe expansion are reported. The calculations were obtained by the numerical solution of the time-averaged forms of the continuity, momentum and thermal energy equations together with equations for the turbulence kinetic energy and its rate of dissipation. For a sudden expansion without swirl, the predictions produced satisfactory agreement with available data for the Nusselt number. In the swirling case, there were no heat transfer measurements available for comparison. However, existing measurements of a swirl flow at an expansion without heat transfer were used to test the validity of the flow field calculations.

The predicted effects of varying the swirl number from zero to 1.0 on the heat transfer behavior are presented for a range of Prandtl numbers from 0.7 to 10. The expected effects of the swirl on the velocity and temperature fields are also reported. The results predict, for example, that the maximum Nusselt number is increased as the swirl number increases and its position moves towards the inlet section. They also show an increase in the Nusselt number as the Prandtl number increases.

*Presently at the Mechanical Engineering Department, Cairo University, Cairo, Egypt.

TABLE OF CONTENTS

	Page
ABSTRACT	ii
TABLE OF CONTENTS	iii
LIST OF ILLUSTRATIONS	iv
NOMENCLATURE	v
1. INTRODUCTION	1
1.1 Background	1
1.2 Previous work	4
1.3 Present work	5
2. ANALYSIS	7
3. PREDICTIONS	13
3.1 Zemanick and Dougall - heat transfer without swirl . . .	13
3.2 Beltagui and MacCallum - swirl without heat transfer . .	15
3.3 Heat transfer with swirl at a sudden expansion	20
4. CONCLUSIONS	32
APPENDIX. Computer program TEACH-Y	A-1
REFERENCES	R-1
DISTRIBUTION	D-1

LIST OF ILLUSTRATIONS

Figure		Page
1	Idealized geometry	3
2	Comparison for heat transfer at a sudden expansion without swirl	12
3(a)	Mean velocity distributions for swirl flow without heat transfer	16
3(b)	Mean velocity distributions for swirl flow without heat transfer (cont'd).	17
4	Development of mean velocity and temperature pro- files for different swirl numbers	21
5	Development of wall shear stress for swirl flow . .	23
6	Effect of swirl on development of local Nusselt numbers	25
7	Effect of swirl on overall heating.	27
8	Effect of Prandtl number on temperature distribu- tions	29
9	Effect of Prandtl number on local Nusselt number. .	31

NOMENCLATURE

Symbol	Definition
C_R	Constant in turbulence model, for correction for stream-line curvature, equation (11)
D	Diameter of pipe downstream of the expansion = $2R_o$
d	Diameter of the pipe upstream of the expansion = $2r$
G	Generation of turbulence kinetic energy K
H	Step height = $(D - d)/2$
H	Enthalpy
K	Turbulence kinetic energy = $\frac{1}{2} \overline{u_i u_i}$
Nu	Nusselt number
Nu_{fd}	Nusselt number of fully developed pipe flow
Pr_l	Molecular Prandtl number
Pr_t	Turbulent Prandtl number
q_w	Wall heat flux
R	Radius of downstream pipe
r	Radial coordinate
Re	Reynolds number; Re_d , based on diameter upstream; Re_D , based on diameter downstream
R_f	Flux Richardson number
S	Swirl number, $\int_0^{r_o} \overline{U} \overline{W} r^2 dr / r_o \int_0^{r_o} \overline{U}^2 r dr$
T_b	Bulk temperature, $\frac{\int \overline{U} T r dr}{\int \overline{U} r dr}$
T_{in}	Inlet temperature

NOMENCLATURE--Continued

Symbol	Definition
T_w	Wall temperature
\bar{U}	Axial mean Velocity
\bar{U}_{av}	Bulk velocity = $\int \rho \bar{U} r dr / \int \rho r dr$
u	Fluctuations of axial velocity
\bar{V}	Radial mean velocity
v	Fluctuations of radial velocity
\bar{W}	Tangential mean velocity
w	Fluctuations of tangential velocity
x	Axial coordinate
X_o	Axial distance downstream from the expansion
y	Transverse coordinate measured from the wall
ϵ	Rate of dissipation of turbulence kinetic energy
κ	von Karman constant for turbulence model, equation (10)
τ_w	Wall shear stress in the axial direction, equation (9)

Subscripts

o	Wall
p	Node point nearest the wall

CHAPTER I

INTRODUCTION

1.1 Background

Current Naval propulsion plants are powered by variations of the Rankine cycle (steam) or the open gas turbine cycle (air and combustion products) plus some diesel engines in small ships. Alternative power systems suggested include the closed gas turbine cycle and cycles involving dissociation of the working fluid in either a Rankine or a gas cycle. These latter two are believed to offer the potential of substantial improvement in the power-to-weight ratio of the propulsion plant. The present and proposed studies consider basic problems in convective heat transfer and flow friction that are important in all of the above.

Convective heat transfer provides the dominant thermal resistance in several components of conventional steam power plants as well as in all heat transfer components in gaseous cycles. For example, heat transfer from the condensing steam to the cooling water in the main condenser of a Naval ship is via the condensation heat transfer coefficient which is high, then conduction conductance through thin tubing of high conductivity, and finally via the moderate heat transfer coefficient of the cooling water flowing through smooth circular tubes. Thus, the overall thermal resistance is dominated by the convective thermal resistance of the cooling water inside the tubes. One can expect significant reductions in tube

length and, therefore, size and weight of the condenser and overall plant if the convective heat transfer coefficient of the cooling water is increased appreciably.

A common geometry recurring in compact Naval propulsion plants is a change in duct size in the primary fluid loop. As a consequence of the upstream plumbing, the fluid is often swirling about the axis in the piping. Heat losses from the primary fluid and thermal stresses in the component depend on the convective heat transfer from the fluid to the component as it undergoes this geometrical transition. The idealized problem is a study of heat transfer in a sudden expansion with swirl flow, the subject of the present report. The same situation also occurs at the entrance to some heat exchanger tubes.

The flow downstream of a sudden expansion consists primarily of a central jet, with or without rotation due to swirl, surrounded by a recirculating donut-shaped vortex induced by the separation as the jet leaves the central tube. This jet gradually spreads as the flow proceeds downstream until it reattaches to the downstream wall and fills the larger tube. Eventually a fully developed velocity profile can be expected to be established if the tube length is sufficiently long. The centrifugal body forces induced by swirl modify the recirculating vortex, the development of the jet and the reattachment location.

Significant enhancement of heat transfer rates generally occurs when fluids are transported through sudden enlargements in pipes (Fig. 1) or duct cross-sections or when they are subjected to angular tangential

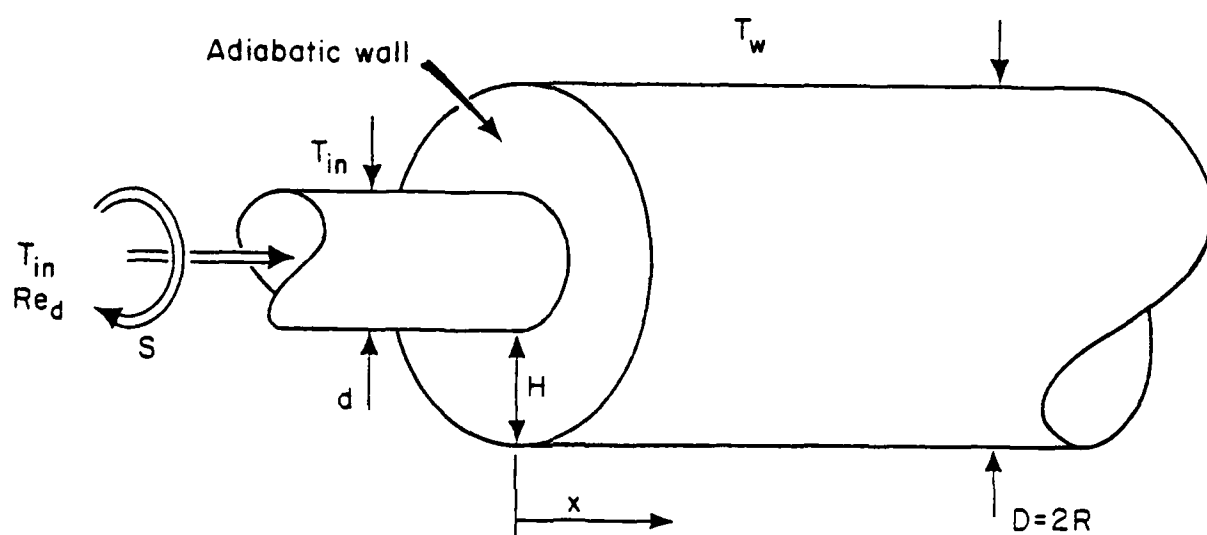


Figure 1. Idealized geometry.

momentum due to twisted tapes or the application of vane-generated swirl. In both cases, the levels of turbulence kinetic energy are increased and the heat transfer rate generally increases as well. High shearing rates created by both separation and swirling effects are associated with high generation rates for the kinetic energy of turbulence; in addition the rate of dissipation of turbulence kinetic energy decreases due to an increase in the length scales. The two effects lead to elevated magnitudes of the kinetic energy of turbulence. All these effects are expected to reduce the thickness of the viscous sublayer through which heat must pass largely by molecular diffusion and so will increase the heat transfer rate.

1.2 Previous work

The problem of heat transfer to separated and reattached subsonic turbulent flows downstream of abrupt pipe expansions has been studied experimentally by a number of investigators such as Ede, Hislop and Morris [1956], Krall and Sparrow [1966] and Zemanick and Dougall [1970]. Reviews of the heat transfer literature for separated and reattached flows are reported by Eckert et al. [1971] and by Fletcher, Briggs and Page [1974]. The experimental data of Krall and Sparrow [1965] for water, and of Zemanick and Dougall [1970] for air are for typical geometries representing axisymmetric abrupt enlargement of tubes. Both teams found a maximum in the local heat transfer coefficient at the assumed point of flow reattachment. Adequate descriptions of wall heat transfer at solid boundaries in regions of separated and

reattached flows have been limited by the lack of a complete solution for the fluid flow field. Spalding [1967] presented a power law relation between the Stanton and the Reynolds numbers for heat transfer from a wall adjacent to a region of separated flow; he employed a one-dimensional model of the flow near a wall. Recently, Chieng and Launder [1980], in calculations of the turbulent heat transfer downstream of an abrupt pipe expansion, found that the Nusselt number is overpredicted by 20% in flows with high Reynolds numbers and that its maximum value occurs about one step height upstream of the calculated reattachment point, relative to the data of Zemanick and Dougall.

For swirling flow, a number of studies have been done to investigate the effect of swirl on heat transfer parameters. Experiments performed by Thomas [Eckert et al., 1971], with swirling air flow in a tube indicated that, for turbulent flow and Reynolds numbers less than 10^5 , the swirl flow transfers heat more efficiently than a non-swirling flow. Zaherdadeh and Jagadish [1975] concluded that an augmentation of up to 80% was obtained, with a constant wall temperature boundary condition, with the use of tangential vane type swirl generators.

1.3 Present work

Calculations of the effects of separation and swirl on heat transfer parameters have rarely been reported and the combined effects of both apparently have not been studied. Thus, we attempt the prediction of such cases in contrast to the "postdiction" usually employed in numerical studies. In the present paper, a calculation method is provided and

is applied for the prediction of flow and temperature fields in the swirling, separated and reattached flow in the vicinity of a sudden expansion of a pipe.

An idealized version of the geometry is shown as Figure 1. The expansion ratio is 2 and the Reynolds number upstream of the expansion is taken as 5×10^4 for the calculations. The effects of swirl on the heat transfer parameters are studied in the range of swirl number from 0.0 to 1.0 and of Prandtl number from 0.7 to 10. For confidence testing, the calculations are compared with the measurements of Zemanick and Dougall [1970] for zero swirl number and those with swirl, but without heat transfer, are compared to the data of Beltagui and MacCallum [1976].

The governing equations and boundary conditions are described in the following section which is ended by a description of the solution procedure. The results are then presented and discussed. The paper ends with a summary of conclusions.

CHAPTER 2

ANALYSIS

Equations representing conservation of mass, energy, turbulence kinetic energy and its dissipation rate plus the momentum equations were solved in axisymmetric coordinates with an extension of the TEACH computer program developed originally by Gosman and Pun [1974]. In the present study, the version of Habib and Whitelaw [1980], which treats double coaxial jet flows, was modified to give predictions of swirl flow downstream of an abrupt pipe expansion and to yield the temperature field and heat transfer parameters by adding the solution of the thermal energy equation.

The equations modeled and the turbulence model are as follows:
continuity,

$$\frac{\partial \bar{U}_j}{\partial x_j} = 0 \quad (1)$$

momentum,

$$\frac{\partial}{\partial x_j} (\rho \bar{U}_i \bar{U}_j + \rho \overline{u_i u_j}) = - \frac{\partial P}{\partial x_i} \quad (2)$$

thermal energy,

$$\frac{\partial}{\partial x_j} (\rho \bar{U}_j H) = \frac{\partial}{\partial x_j} \left(\frac{\mu_{eff}}{\sigma_H} \frac{\partial H}{\partial x_j} \right) \quad (3)$$

turbulence kinetic energy,

$$\frac{\partial}{\partial x_j} (\rho \bar{U}_j k) = \frac{\partial}{\partial x_j} \left(\frac{\mu_{eff}}{\sigma_k} \frac{\partial k}{\partial x_j} \right) + G - \rho \epsilon \quad (4)$$

and dissipation of turbulence kinetic energy

$$\frac{\partial}{\partial x_j} (\rho \bar{U}_j \epsilon) = \frac{\partial}{\partial x_j} \left(\frac{\mu_{eff}}{\sigma_\epsilon} \frac{\partial \epsilon}{\partial x_j} \right) + C_1 \frac{\epsilon}{k} G - C_2 \frac{\epsilon^2}{k} \quad (5)$$

$$\text{with } \mu_{eff} = \mu_l + \frac{C_\mu \rho k^2}{\epsilon} \quad (6)$$

$$G = -\rho \overline{u_i u_j} \frac{\partial \bar{U}_i}{\partial x_j}, \quad k = \overline{u_i u_i} / 2$$

and

$$-\rho \overline{u_i u_j} = \mu_{eff} \left(\frac{\partial \bar{U}_i}{\partial x_j} + \frac{\partial \bar{U}_j}{\partial x_i} \right) - \frac{2}{3} \rho k \delta_{ij}$$

$$\text{where } \delta_{ij} = 0 \text{ if } i \neq j \text{ and } \delta_{ij} = 1 \text{ if } i = j. \quad (7)$$

Fluid properties were idealized as constant except in some cases with air where the density was allowed to vary due to pressure variation.

In addition to the set of equations listed above, the following inlet and boundary conditions are considered. In the case of non-swirling flows, data for fully developed pipe flow were taken as initial values for mean velocity and turbulence kinetic energy. The inlet dissipation rate was then determined from its model,

$$\epsilon = c_u \frac{K^{3/2}}{\ell} \quad (8)$$

where ℓ is the length scale that characterizes the energy containing eddies, taken as $\ell = 0.03 r_o$.

For swirl, the initial axial and tangential mean velocities were interpolated from the data of Habib [1980]. The turbulence kinetic

energy was taken as a function of the total mean kinetic energy and the dissipation rate was determined via equation (8) with λ assumed to be given as $r_0 (0.03 + 0.07S)$.

All axial gradients, $\partial/\partial x$, were presumed zero at the exit plane of the tube well downstream. Axial symmetry was specified so $\bar{V} = 0$ and the radial gradients of all other quantities were zero at the centerline. No slip and impermeable wall conditions were specified on all solid surfaces.

Wall functions [Launder and Spalding, 1972] corresponding to the dependent variables were taken as

$$\tau_w = \frac{\mu_\ell \bar{U}_p}{y_p} \frac{y_p^+}{U_p^+} \quad (9)$$

where $U_p^+ = \frac{1}{\kappa} \ln Ey_p^+$ and $y_p^+ = C_\mu^{1/4} K_p^{1/2} y_p / \nu_\ell$

$$\text{and} \quad q_w = \frac{\mu_\ell (H_w - H_p)}{y_p} \frac{y_p^+}{U_p^+ + P_f} \quad (10)$$

$$\text{where } P_f = C_f \left(\frac{Pr_{,\ell}}{Pr_{,t}} - 1 \right) \left(\frac{Pr_{,t}}{Pr_{,\ell}} \right)^{1/4}$$

The value of the kinetic energy of turbulence near the wall, K_p , is calculated from the transport equation for K with the flux of energy to the solid wall set to zero. The corresponding value of ϵ was calculated from equation (8) with $\lambda = C_\mu^{1/4} \kappa y_p$.

The constants used in the above equations are in accord with those of Khalil and Whitelaw [1974] and Pope and Whitelaw [1976]. They are summarized as follows:

$$\begin{aligned} C_\mu &= 0.09, & \sigma_K &= 1.0, & \sigma_\epsilon &= 1.22, & \sigma_H &= 0.9, & C_1 &= 1.45, \\ C_2 &= 1.9, & C_f &= 9.24, & \kappa &= 0.42, & E &= 9.8 \end{aligned} \quad (10)$$

Modification of C_1 to account for streamline curvature is described in Section 3.2 later.

The solution procedure described by Patankar and Spalding [1972] was used to solve the above equations. From trial values of the pressure distribution, the momentum equations can be solved to obtain an estimate of the velocity field at the first iteration. However, there is no guarantee that the resultant velocity field will satisfy the continuity equation, therefore, after each calculation over the solution domain, adjustments are made to the pressure and velocity fields to satisfy continuity. The procedure is repeated until convergence is obtained. The energy equation is then solved and the temperature field is presented.

Most of the computations were done with a grid of 25 x 18 nodes with more points concentrated near the walls and regions of separation and high velocity gradients. The computer time (per iteration per grid node) using the CDC CYBER 175 was 9.5×10^{-4} Sec to solve the velocity field and 1.2×10^{-4} Sec to obtain the temperature field. (These time estimates typically corresponded to \$24/run and \$6/run, respectively, at University rates). The storage requirements of the program were 37,000 octal words.

A grid independence test was conducted during the comparisons to the data of Zemanick and Dougall [1970]. It showed that an increase in the number of nodes from 20×17 to 27×21 affects the predicted Nusselt number only in the region of its maximum (see Figure 2) and then less than three percent. The effect was negligible in the downstream region. For most of the predictions presented in the next section a grid of 25×18 nodes was employed so they are expected to have better numerical accuracy than the former case.

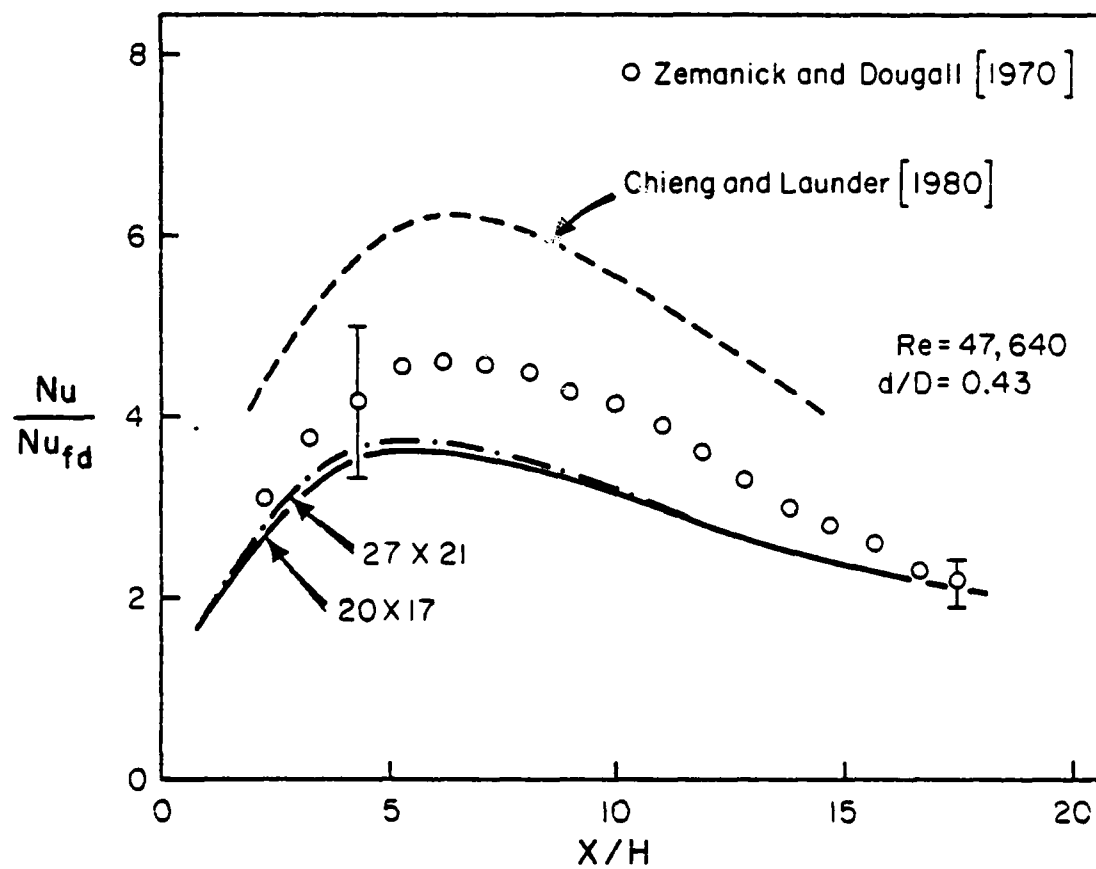


Figure 2. Comparison for heat transfer at a sudden expansion without swirl.

CHAPTER 3

PREDICTIONS

In this section results from the computer program are first compared to the available data to test its validity. Then, the predictions of the separated flow with both swirl and heat transfer are presented.

3.1 Zemanick and Dougall - heat transfer without swirl

The results are first compared with the experiment of Zemanick and Dougall [1970] for zero swirl. Since inlet velocity profiles were not presented, the initial conditions were taken as those of fully developed pipe flow in the smaller tube. In the run chosen for comparison, the expansion ratio was 0.43 and the Reynolds number calculated downstream from the expansion was 47,800. In the experiment resistive heating was employed so the appropriate thermal boundary condition would be a specified wall heat flux. To correspond with the procedure of the present program, the wall temperature distribution which was measured was entered as the thermal boundary condition and the wall heat flux was calculated via equation (10).

As noted by Zemanick and Dougall [1970] there were some difficulties with their experiment so it is not ideal for a close comparison, but it is one of the few with data readily available. Axial conduction in the tube was significant and the thickness of the copper electrode at the expansion extended about a step height in the downstream direction. In addition it may be noticed that their correlation of local

Nusselt numbers in the fully developed region downstream is about 15% higher than commonly accepted values [McEligot, Magee and Leppert, 1965]. Unfortunately, quantitative estimates of the experimental uncertainties [Kline and McClintock, 1953] were not presented. If one assumes an uncertainty of 1°C in measuring the wall temperature, typical of premium grade thermocouple wire, it can be shown that this effect alone would lead to an uncertainty of about twenty percent in the Nusselt number near the entry and approximately five percent downstream; these estimates are shown by brackets on Figure 2. Thus, it is best to restrict the comparison to trends rather than absolute magnitudes.

Figure 2 shows a comparison between the calculated and measured distributions of Nusselt numbers; the curves represent the numerical predictions. It is shown that the agreement is generally good in the upstream and downstream locations with the present calculations underpredicting the maximum Nusselt number by about 20%. The location of the maximum Nusselt number is found to be one step height upstream from the corresponding peak in the experiments. By examination of the predicted velocity distributions it may also be found that the calculated maximum Nusselt number occurs two step heights upstream from the calculated reattachment point. This direction was also indicated by Chieng and Launder [1980]; however, they indicate the difference in location to be one step height only.

The discrepancy between the calculations and the experiment may be attributed partly to the numerical accuracy in the calculation

procedure. Increasing the number of grid points to reduce effects of the numerical diffusion leads to a slight increase in Nusselt number in the entry region as shown on Figure 2. However, as noted earlier, the increase in the number of nodes from 20×17 to 27×21 gives a change of less than 3% which is essentially negligible for the present purposes.

3.2 Beltagui and MacCallum - adiabatic flow with swirl

For swirl, data with heat transfer are not available to compare to predictions; however, the adiabatic measurements of Beltagui and MacCallum [1976] were considered to test the flow field calculations and to provide guidance. It is expected that when the model provides predictions which are satisfactory for the flow field calculations, then the heat transfer calculations which depend on them will consequently be reasonable too.

Predictions were calculated for the conditions of the experiment by Beltagui and MacCallum [1976] with $Re = 2 \times 10^5$, $S = 0.67$ and $d/D = 0.413$ as expansion ratio. Their measurements do not include inlet velocity profiles; therefore initial values for the present calculations were interpolated to $S = 0.67$ from the data of Habib [1980].

Results based on the standard $K-\epsilon$ model of Section 2 are shown as curves with centerline markings (dash-dot) in Figure 3(a) for axial mean velocity profiles and Figure 3(b) for circumferential mean velocity distributions. Dashed lines represent the experimental observations. It should be noticed that the ordinate scale changes as effects decay downstream.

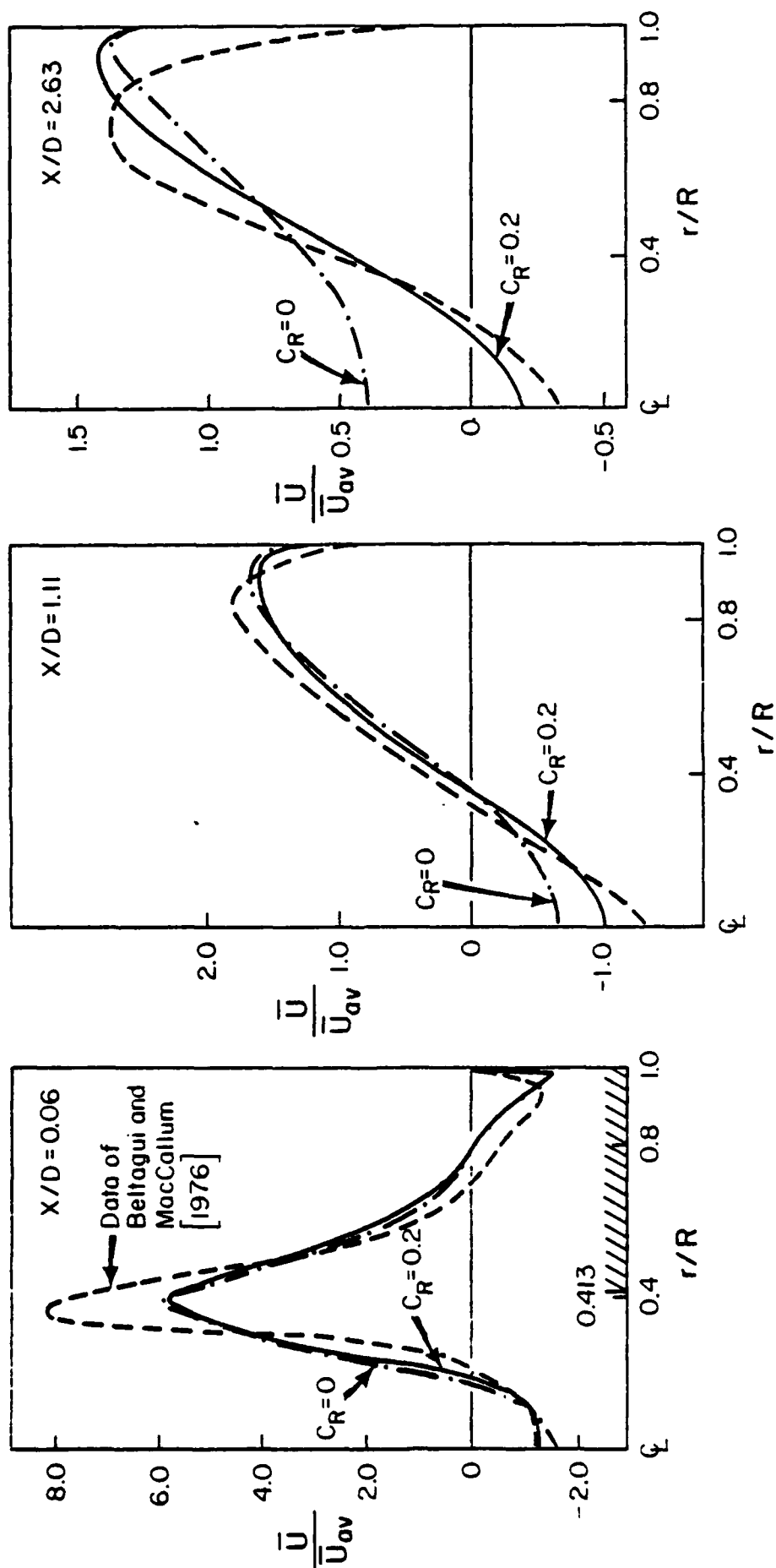


Figure 3(a). Mean velocity distributions for swirl flow without heat transfer, $S \approx 0.67$, $Re = 2 \times 10^5$ and $d/D = 0.413$ as flow parameters.

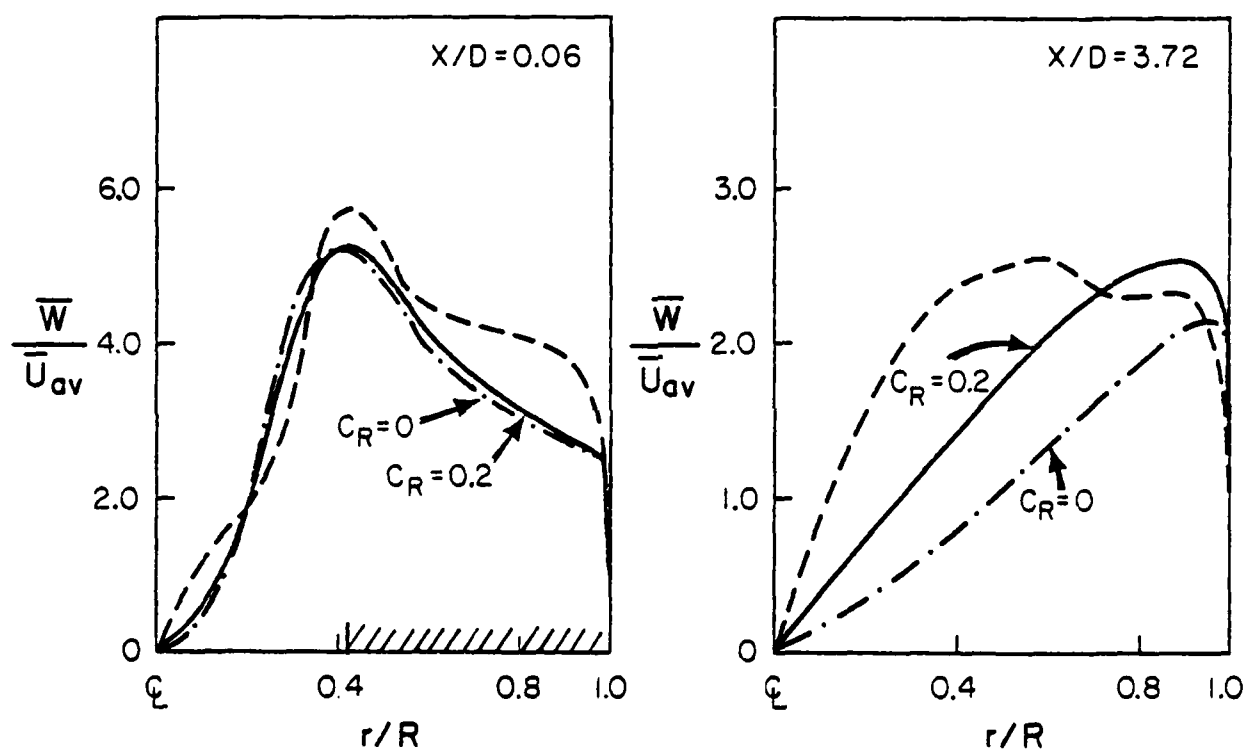


Figure 3(b). Mean velocity distributions for swirl flow without heat transfer (cont'd).

One effect of this relatively high swirl is that the central jet rapidly takes the form of a circular sheet which moves radially outward and attaches to the wall of the outer tube in a short distance. Consequently, the surrounding vortex becomes significantly smaller in size than without swirl and is seen as a small reversed flow region at only the first axial location. Along the centerline of the larger tube a reversed flow also appears showing the existence of another recirculating vortex of size comparable to the diameter of the smaller tube. The qualitative trends are in agreement with the data. The axial velocity profiles agree well except near the centerline where the vortex is predicted to be shorter than measured (e.g., compare centerline velocities at $X/D = 2.63$). Also the tangential velocity in the central region is predicted to decay more quickly than observed.

The discrepancies are partially explained by Khalil and Whitelaw [1974] and Habib and Whitelaw [1980], who showed that the standard $K-\epsilon$ model often yields underpredicted lengths for the central recirculation zones of swirling flows. The work of Pope and Whitelaw [1976] for flows behind a baffle and of Habib and Whitelaw [1981] for confined flows with a sudden expansion indicates that the dissipation equation is the weakest of the governing equations since its modelling is only based on assumptions. As shown by Bradshaw [1973], body forces due to streamline curvature can have a strong effect on turbulence and the equations of turbulence models should account for these effects. Recently, Rodi [1979] and Morse [1980] found that it is essential to

correct one of the empirical constants in the dissipation equation as a function of Richardson numbers to achieve agreement with experiments.

To improve the present calculations, we replaced C_1 , the empirical constant in the dissipation equation, by $C_1(1 + C_R R_f)$ where R_f is the flux Richardson number [Bradshaw, 1973]

$$R_f = \frac{2 \frac{\bar{W}}{r} \frac{\partial \bar{W}}{\partial r}}{\left(\frac{\partial \bar{U}}{\partial r}\right)^2 + \left(\frac{\partial \bar{W}}{\partial r}\right)^2} \quad (11)$$

The use of $C_R = 0.2$ was found to increase the length of the recirculation zone from about 1.7D to 3.6D. This value was chosen to provide the best agreement with the measured size of the central recirculation zone.

Predictions with $C_R = 0.2$ are presented as solid curves in Figure 3. The axial velocity profiles show considerably better agreement with the data in the central recirculating region, as would be expected from the manner of adjustment, and slightly better agreement near the wall. The predicted circumferential velocity distribution is also improved near the wall, the region with the greatest effect on the heat transfer, but as the centerline is approached the values appear to be under-predicted. Comparison of the predicted velocities with $C_R = 0$ and $C_R = 0.2$ shows that modifying C_1 with this functional dependence on R_f tends to decrease the rate of diffusion in the downstream sections and to suppress the development of the jet.

3.3 Heat transfer with swirl at a sudden expansion

Calculations of heat transfer to a swirling flow were made after an abrupt enlargement of $D/d = 2$ for an inlet Reynolds number (Re_d) of 50,000 and with constant wall temperature imposed after the expansion. It was idealized that there was no heat transfer through the annular step between the inner and outer tubes. For flows at the different swirl numbers studied the inlet distributions of velocities and kinetic energy of turbulence were interpolated from the data of Habib [1980]. The effects of varying swirl number and Prandtl number were examined separately.

Effects of swirl were studied with the Prandtl number taken as 0.7 as for common gases. Predictions are shown in Figures 4 through 7. Figure 4, presenting the development of velocity and temperature distributions, provides information which helps understanding the later figures. On these figures the solid curves represent the reference case: zero swirl.

In Figure 4 the velocity profiles show that at $S = 0.1$ the flow is only slightly modified, at $S = 0.4$ there are significant differences and for $S = 1$ the general pattern of the flow changes. These runs might be considered as showing low, medium and high swirl, respectively. As the swirl (or angular momentum) increases, the reattachment point of the separated region in the corner moves successively closer to the entrance and the central jet spreads more rapidly towards the wall. After a short distance the velocity profile for $S = 0.4$ resembles a

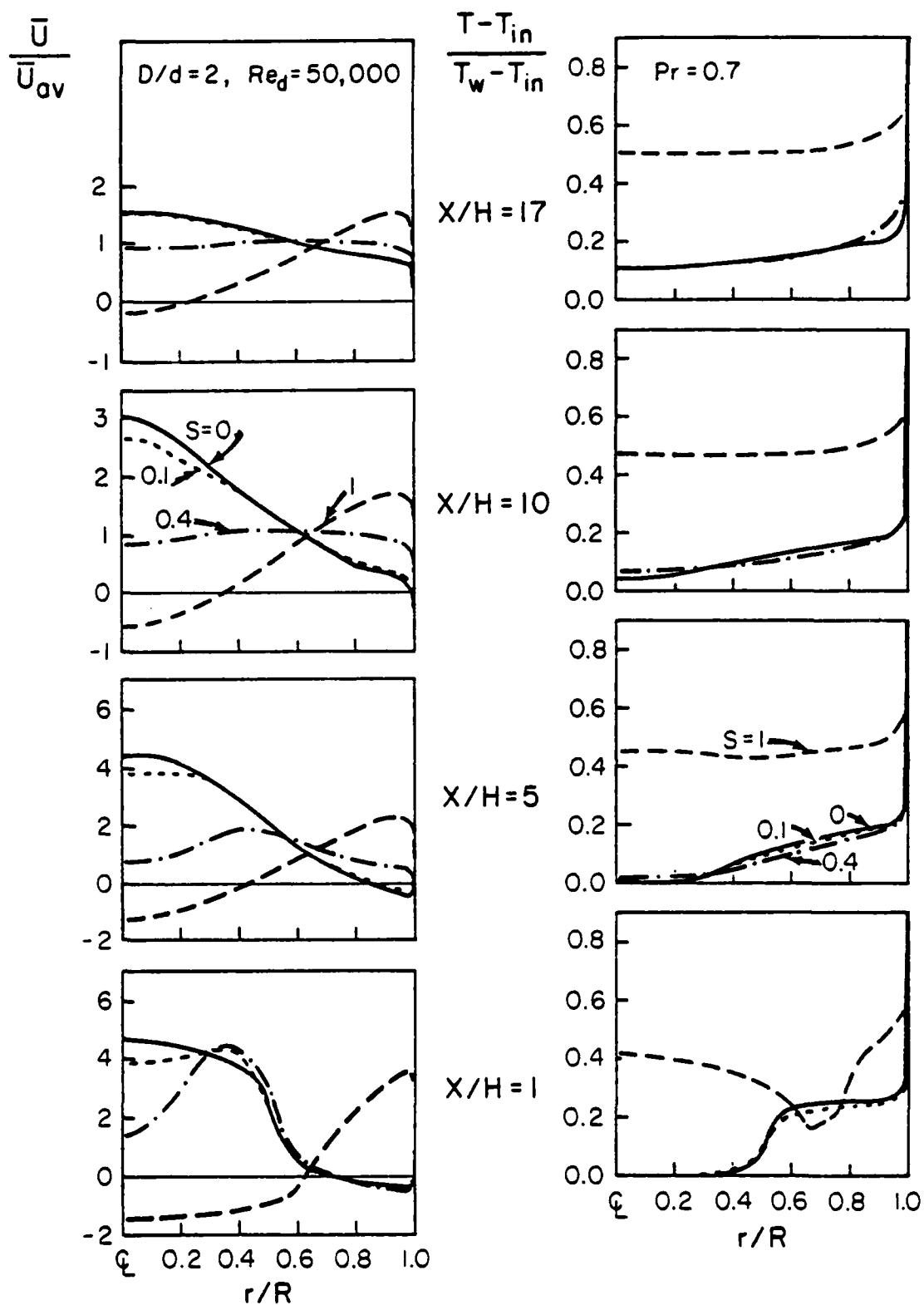


Figure 4. Development of mean velocity and temperature profiles for different swirl numbers.

plug flow. The velocity near the heated wall increases with S in this entry region.

At $S = 1$ the flow pattern resembles that of Beltagui and MacCallum [1976] shown earlier. For this high swirl number the flow exhibits a long central recirculation zone while the outer recirculation zone is decreased to $0.13H$. Flow development is delayed as the central jet becomes a wall jet with the reversed flow at the centerline persisting to beyond $X/H = 17$. These features are also demonstrated by Habib [1980].

The corresponding variation of the non-dimensional wall shear stress or friction factor is shown on Figure 5 (note the change of scale for $S = 1$). Negative values occur due to the reversed flow near the wall. The value of zero indicates the location of the reattachment point or position where the dividing mean streamline meets the wall. As S increases this point progresses upstream as noted from examination of the velocity distribution; the points of maximum shear stress likewise move upstream. The magnitudes of the extremes also increase with swirl; an effect of the centrifugal forces apparently is to drive the higher velocity central flow towards the wall, thus steepening the velocity gradient. For fully developed, turbulent flow in a tube at $Re_D = 25,000$ the friction factor is expected to be about 0.006 [Kays, 1966] so all the flows must go considerably further downstream before becoming fully developed.

The temperature profiles in Figure 4 show approximately isothermal zones across the recirculating regions, thereby demonstrating high transport

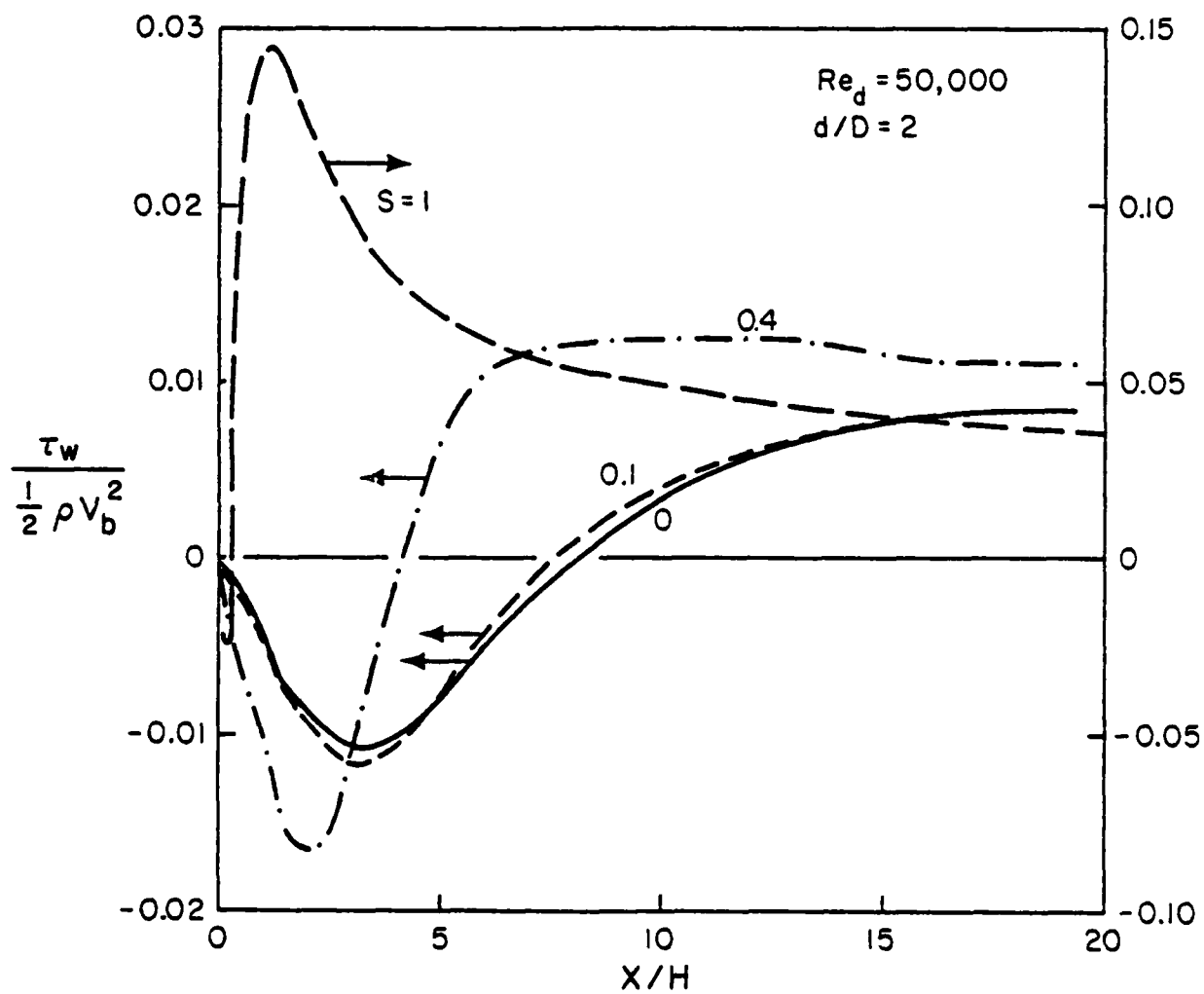


Figure 5. Development of wall shear stress for swirl flow.

rates due to the turbulent mixing in these regions. For the range $S \leq 0.4$ there is only a slight change in temperature distributions as the swirl is increased.

The interesting case is for high swirl flow. Within 5 step heights (or $1.25 D$) the central recirculating flow is approximately isothermal. By $X/H = 1$ this reversed flow has carried thermal energy forward from further downstream and, thereby, has raised the centerline temperature substantially. The small recirculating region near the wall has done the same for that region, giving the appearance of a cooled wake at an intermediate radius. However, before $X/H = 5$ the central region has expanded and has eliminated the wake appearance in the temperature distribution.

Predicted local Nusselt numbers are shown in Figure 6 normalized by

$$Nu_{fd} = 0.020 Re^{0.8} Pr^{0.4}$$

a correlation for fully developed turbulent flow with a constant wall temperature [Kays, 1966]. As for the wall shear stress, increasing swirl increases the maximum value and moves it upstream towards the entry. The higher velocity gradient corresponds to flow at a higher Reynolds number so the viscous layer, which dominates the thermal resistance, is thinner and the Nusselt number is increased. Comparison to Figure 5 shows that for each swirl number the maximum Nusselt number occurs near the point of reattachment, which was shown earlier to move upstream as swirl increases.

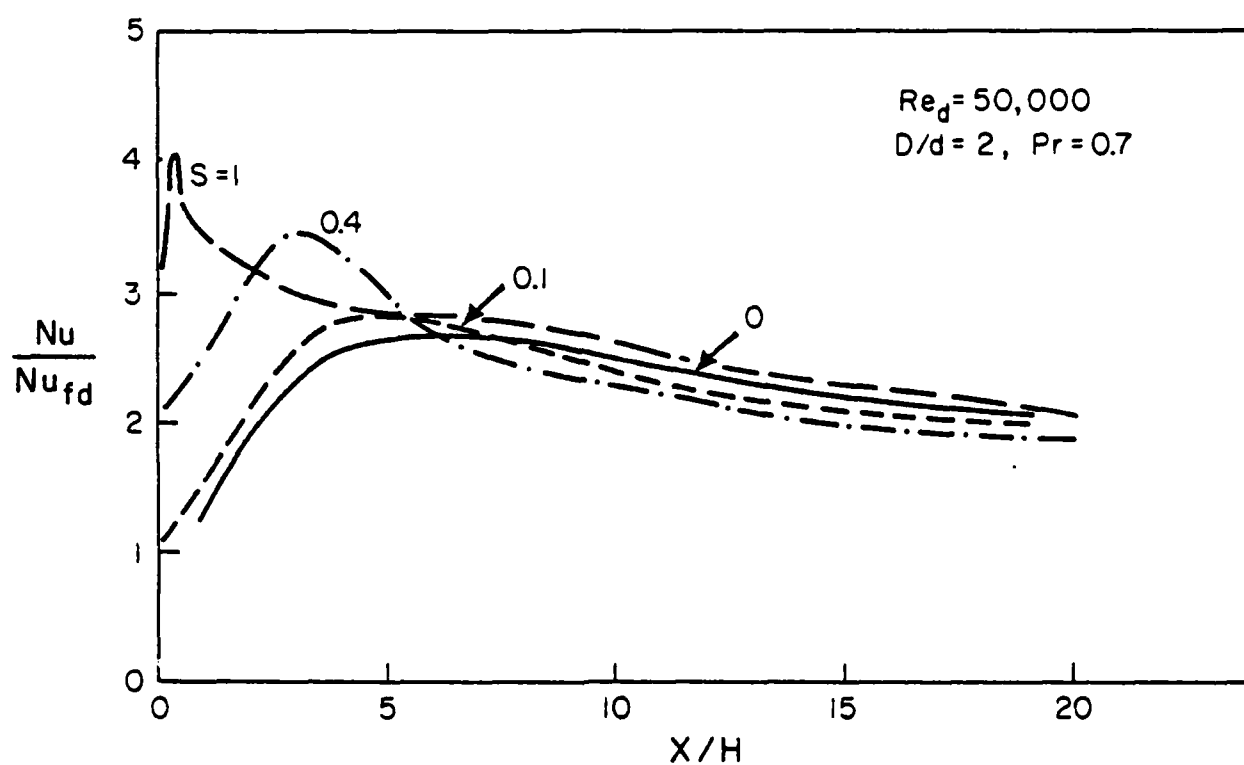


Figure 6. Effect of swirl on development of local Nusselt numbers.

For the high swirl case, the increase in Nu_{max} due to the combined effects of separation at the annular step and swirl is four times while for separation alone the improvement is 2.5, relative to fully developed flow. Thus, the major increase is due to the separation. Further downstream, the low and moderate swirl cases show a slight decrease in Nusselt number as swirl number increases. This result may be the consequence of swirl reducing the length of the outer separated zone so that the development of the normal tube flow has progressed further at a given location, i.e., for given X , $X - X_{reattachment}$ increases with S . For $S = 1$ the strong wall jet phenomenon continues to dominate the velocity profile and, apparently, maintains a slightly higher Nusselt number than for zero swirl.

For applications such as heat exchangers, the designer is interested in the resulting bulk temperature variation of the fluid as it is heated (or cooled). Figure 7 presents this information and it is seen that an effect of swirl is to increase the bulk temperature and its rate of increase slightly. After viewing the temperature profiles, it may seem surprising that the increase is not greater for high swirl. The difficulty is that, though the temperature is approximately uniform, the velocity changes sign in the large reversed flow in the central region. In calculating the bulk temperature via its definition ($\int \bar{U} T dr / \int \bar{U} dr$) the enthalpy flow rate there is subtracted from the enthalpy flow rate in the positive direction giving a net value which is smaller than expected. Therefore, while local heat transfer rates are increased substantially by swirl the overall improvement is not proportionally as large.

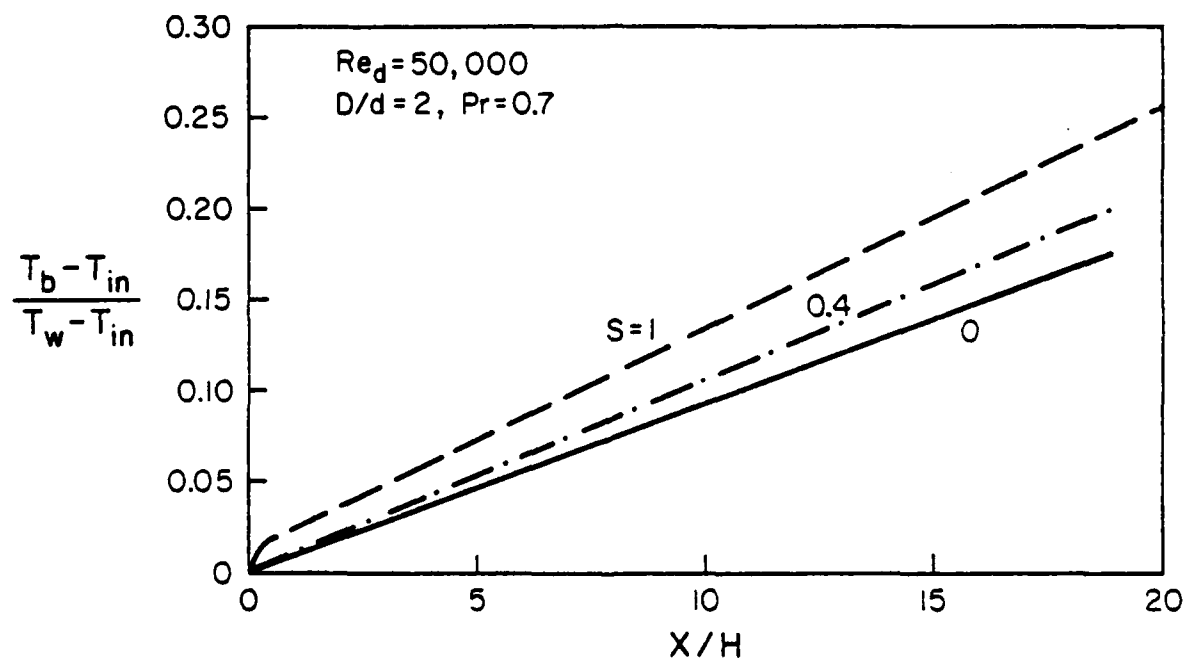
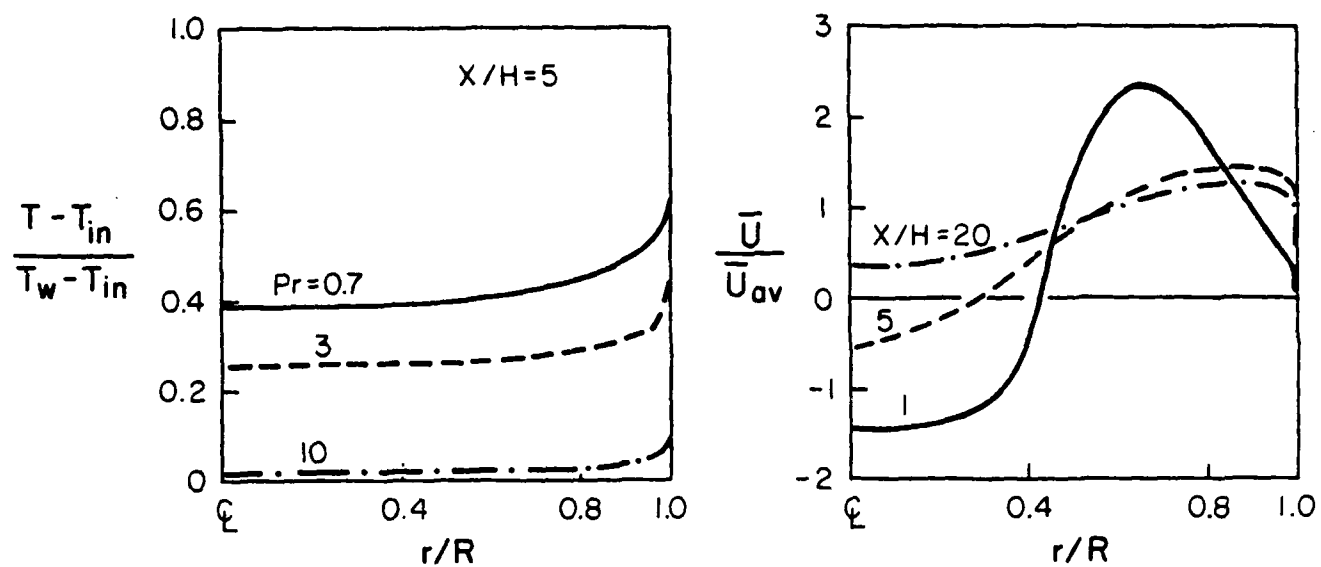


Figure 7. Effect of swirl on overall heating.

Predictions of the effects of Prandtl number on heat transfer were calculated for $S = 0.7$, again at $Re_d = 50,000$ and $D/d = 2$. Examination of the expected velocity profiles in Figure 8 shows this situation to be a high swirl case with a substantial recirculating vortex in the central region. In comparison to the profile for $S = 1$ at $X/H = 1$ in Figure 4, one finds the same shape except the maximum does not fall as close to the wall in this case with lower swirl. Lower circumferential momentum at the entry causes the main streamlines of the annular jet to have less rapid divergence from the axis.

Temperature profiles were calculated for $Pr = 0.7, 3$ and 10 , corresponding to common gases and liquid water at about 60°C and 10°C , respectively. Results are also shown on Figure 8. The general behavior is in agreement with the earlier predictions for $S = 1$.

At each axial location the temperature profiles have the same general shape for all Prandtl numbers. Only the magnitudes change significantly. Thus, the total thermal energy transferred to the flow is greater as the Prandtl number decreases. The similarity of the shapes may be taken as an indication that convection dominates the thermal energy transfer processes in these regions despite the increased thermal conductivity implied by lower Prandtl numbers. The levels of the curves then depend on the heat fluxes at the wall where the thermal conductivity does dominate the thermal resistance. Thus, accurate prediction of heat transfer parameters requires accurate knowledge of the behavior of the viscous layer in this flow as well as in simpler ones.



$Re_d = 50,000 \quad D/d = 2 \quad S = 0.7$

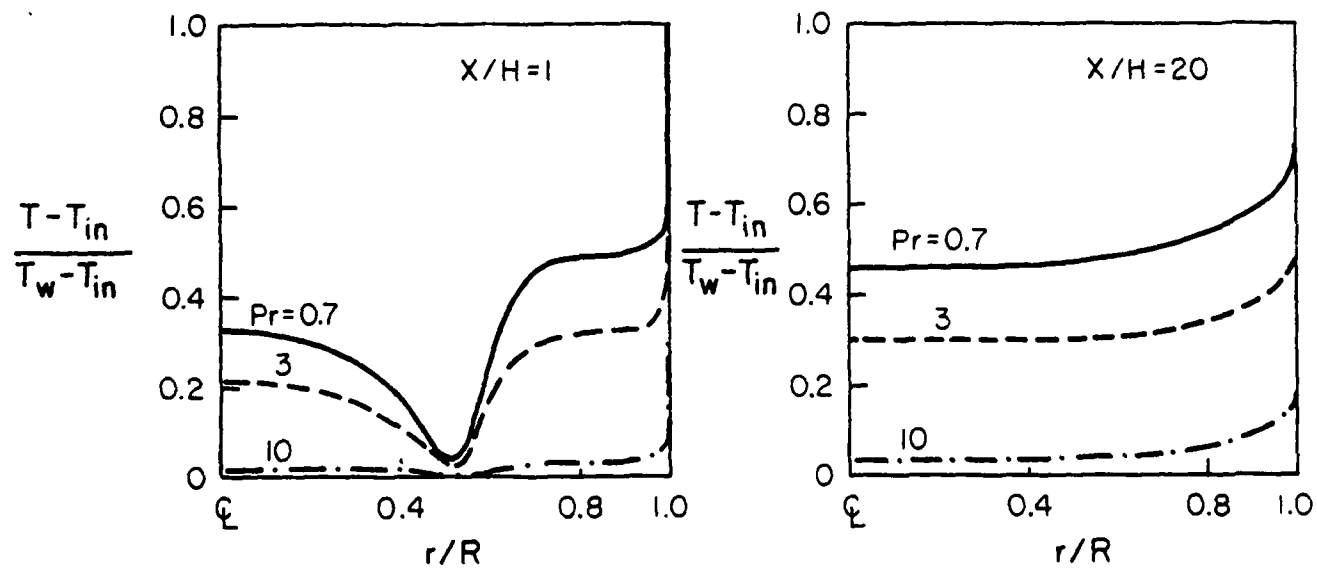


Figure 8. Effect of Prandtl number on temperature distributions.

The axial distribution of local Nusselt numbers is presented as Figure 9; the curve for $Pr = 0.7$ is consistent with the trends of Figure 6 earlier. Again, as with the temperature profiles, the shape of the Nusselt number distribution is primarily dependent on the flow parameters-- Re , S and D/d --and is relatively independent of the Prandtl number. However, the level or magnitude of the results increases as the Prandtl number increases so, as a general conclusion, one may note that the local Nusselt numbers increase with the Prandtl number as in most flows.

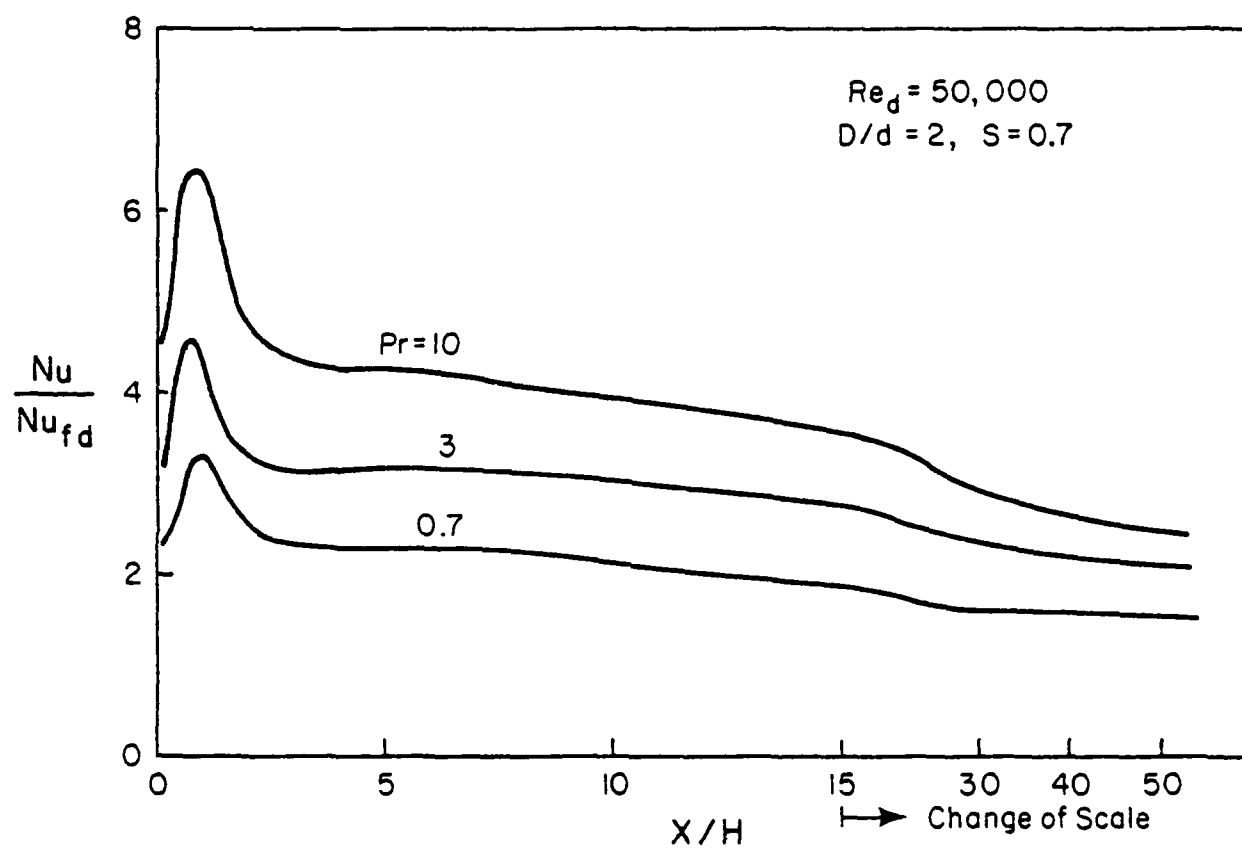


Figure 9. Effect of Prandtl number on local Nusselt number.

CHAPTER 4

CONCLUSIONS

The following important conclusions can be extracted from the preceding results:

- 1) For heat transfer without swirl, generally good agreement is obtained between measured and calculated Nusselt numbers.
- 2) For an adiabatic flow with swirl, predictions could be obtained in agreement with available data by modifying the turbulence model to account for effects of streamline curvature.
- 3) For swirl flow with heat transfer, (a) the maximum local Nusselt number is predicted to increase and its location moves towards the entry as the swirl number increases, and (b) the local Nusselt number increases as the Prandtl number increases.

APPENDIX. COMPUTER PROGRAM*

1. Comments concerning parameters used in Block data of Teach T.CDC

IGET: This parameter indicates continuation of calculations
 from previous output saved on magnetic tape

 ≡1 Does not read or write any output

 >1 Writes data on tape 8

 >2 Reads from Tape 7 and writes on Tape 8

IHT Parameter controls heat transfer calculations

 ≡1 There is a heat transfer calculation (the thermal
 energy equation is solved)

 ≡0 No heat transfer calculations

ICP Parameter used to restrict the program to calculations for a
 constant property fluid

 ≡0 Flow field calculations only

 ≡1 Energy equation is solved alone provided that the flow
 is known from a previous set of iterations. In this
 case (i.e., ICP = 1) IHT should be set to 1 also.

 The program may consider changes in density when the
 fluid is air. For this case set IHT = 1 and ICP = 0.

IABN Defines North wall (i.e., larger tube) as adiabatic

 ≡0 There is heat transfer through the North wall

 ≡1 There is no heat transfer through the North wall

IABW Sidewall (end wall) boundary situation

 ≡0 There is heat transfer through the side wall.
 (This option was not tested.)

 ≡1 There is no heat transfer through the side wall

*Questions concerning the details of the program should be directed to
Dr. M. A. Habib, Power Section, Mechanical Engineering Department, Cairo
University, Cairo, Egypt.

CRF	Constant C_R used with equation (11) for streamline curvature correction. (It is only useful in the swirl cases.)
$\equiv 0$	There is no correction
$\equiv 0.2$	There is a correction (with $C_R = 0.2$)
MAXIT	Maximum iterations allowed. (It will write the results if IGET>2)
INDPRI	Defines the number of iterations after which the program shows a sample of the calculations
PO	Atmospheric pressure, N/m^2
CP1	Specific heat, $J/Kg\ C^\circ$
GASCON	Universal gas constant = $8314\ J/Kgmole\ C^\circ$
WFLUID	Molecular weight, $Kg/Kgmole$
COND	Thermal conductivity, $Watt/m\ C^\circ$
NOTAIR	
$\equiv 0$	The fluid is air or a comparable gas
$\equiv 1$	The fluid is not air and the properties for the fluid must be inserted. These are identified as CPFL, CONDFL, VISFL, DENFL)
PRLAM, PRH	Laminar and turbulent Prandtl numbers
DENFL	<div style="display: inline-block; vertical-align: middle; font-size: 3em; line-height: 1;">}</div> The properties of the fluid to be used if it is not considered to be air. (NOTAIR should be equal to 1 to consider these.)
CPFL	
VISFL	
CONDFL	
ICHF	Indicates whether there is a constant heat flux boundary condition along the larger tube.
$\equiv 0$	Not constant heat flux; the program needs a specified wall temperature distribution
$\equiv 1$	Constant heat flux boundary condition

QADD Wall heat flux in the case of a constant heat flux boundary condition, J/m^2s . (To be used only if ICHF = 1)

TIN Inlet temperature, K°

SWNO Swirl number, defined as the axial flow of tangential momentum divided by the axial momentum rate, $\int_0^R \bar{U} \bar{W} r^2 dr / R \int_0^R \bar{U}^2 r dr$, where R is the nozzle radius.


$\equiv 0$ No swirl

\equiv any value Magnitude of swirl number

UFUIN The maximum inlet velocity (on the centerline); important only if SWNO = 0. The program then treats the inlet as fully developed pipe flow and UFUIN is the value at the centerline.

RLARGE }
& }
DNOZLE }

Geometry



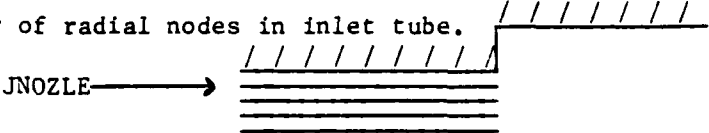
IDATA Parameters specify if the input velocities, turbulence kinetic energy and dissipation will be supplied via READ statements or will be calculated by the program as fully developed pipe flow.

$\equiv 0$ For swirl number = 0 (SWNO = 0)

$\equiv 1$ For others. In this case, at the University of Arizona Computer Center, the program Teach.Vel should be run first; its output should be saved on Tape 4; then the present program is run and it will automatically read \bar{U} , \bar{W} , K , ϵ from Tape 4.

NI, NJ Number of nodes in x and y directions, respectively

JNOZLE Number of radial nodes in inlet tube.



X Locations of nodes in the x-direction

Y Location of nodes in the radial direction (starts from centerline)

TWALN North wall temperature, K

TWALW Side wall temperature, K

2. Program listing (following pages)

1	1	DATA	DATA
2	2	DATA	DATA
3	3	DATA	DATA
4	4	DATA	DATA
5	5	DATA	DATA
6	6	DATA	DATA
7	7	DATA	DATA
8	8	DATA	DATA
9	9	DATA	DATA
10	10	DATA	DATA
11	11	DATA	DATA
12	12	DATA	DATA
13	13	DATA	DATA
14	14	DATA	DATA
15	15	DATA	DATA
16	16	DATA	DATA
17	17	DATA	DATA
18	18	DATA	DATA
19	19	DATA	DATA
20	20	DATA	DATA
21	21	DATA	DATA
22	22	DATA	DATA
23	23	DATA	DATA
24	24	DATA	DATA
25	25	DATA	DATA
26	26	DATA	DATA
27	27	DATA	DATA
28	28	DATA	DATA
29	29	DATA	DATA
30	30	DATA	DATA
31	31	DATA	DATA
32	32	DATA	DATA
33	33	DATA	DATA
34	34	DATA	DATA
35	35	DATA	DATA
36	36	DATA	DATA
37	37	DATA	DATA
38	38	DATA	DATA
39	39	DATA	DATA
40	40	DATA	DATA
41	41	DATA	DATA
42	42	DATA	DATA
43	43	DATA	DATA
44	44	DATA	DATA
45	45	DATA	DATA
46	46	DATA	DATA
47	47	DATA	DATA
48	48	DATA	DATA
49	49	DATA	DATA
50	50	DATA	DATA
51	51	DATA	DATA
52	52	DATA	DATA
53	53	DATA	DATA
54	54	DATA	DATA
55	55	DATA	DATA
56	56	DATA	DATA
57	57	DATA	DATA
58	58	DATA	DATA
59	59	DATA	DATA
60	60	DATA	DATA
61	61	DATA	DATA
62	62	DATA	DATA
63	63	DATA	DATA
64	64	DATA	DATA
65	65	DATA	DATA
66	66	DATA	DATA
67	67	DATA	DATA
68	68	DATA	DATA
69	69	DATA	DATA
70	70	DATA	DATA
71	71	DATA	DATA
72	72	DATA	DATA
73	73	DATA	DATA
74	74	DATA	DATA
75	75	DATA	DATA
76	76	DATA	DATA
77	77	DATA	DATA
78	78	DATA	DATA
79	79	DATA	DATA
80	80	DATA	DATA
81	81	DATA	DATA
82	82	DATA	DATA
83	83	DATA	DATA
84	84	DATA	DATA
85	85	DATA	DATA
86	86	DATA	DATA
87	87	DATA	DATA
88	88	DATA	DATA
89	89	DATA	DATA
90	90	DATA	DATA
91	91	DATA	DATA
92	92	DATA	DATA
93	93	DATA	DATA
94	94	DATA	DATA
95	95	DATA	DATA
96	96	DATA	DATA
97	97	DATA	DATA
98	98	DATA	DATA
99	99	DATA	DATA
100	100	DATA	DATA

[illegible]

05/19/81 12.05.45

FILE 4.005213

74116 717=0 12A3E

СЛУЖБА РАЈИ

[illegible]

[illegible]


```

1337:      U(1,J)=UFUIN**1.5/(ALAMDA**LARGE)
1338:      HIN=CP*HIN
1339:      DO 64 J=1,NIM1
1340:      IF (J.GT.JNOZLE) GO TO 2117
1341:      U(1,J)=UFUIN*(1-ABS(Y(J)))/(Y(JNOZLE+1))**AB
1342:      V(1,J)=TEFTIN*(1+CONST1*((ABS(Y(J))/(ONOZLE/2))**AH2))
1343:      F(1,J)=F(1,J)**1.5/(ALAMDA**LARGE)
1344:      RI=ONOZLE/2
1345:      ALP=RI**10/1-0.08*(Y(1)/RI)**2-0.06*(Y(J)/RI)**4)
1346:      ALP=CMU**0.75*ALP
1347:      ALP=0.03*RI
1348:      ALP=ALP
1349:      DATA OF CHATUKVEFI (1953)
1350:      U(1,J)=UFUIN
1351:      F(1,J)=F(1,J)*UFUIN**2
1352:      VIS(1,J)=DEN*(1.1)*TE(1,J)**1.5/ALP
1353:      OFN(1,J)=DENF
1354:      H(1,J)=HIN
1355:      GO TO 3
1356: 2117 CONTINUE
1357:      F(1,J)=SMALL
1358:      ED(1,J)=SMALL
1359:      U(1,J)=SMALL
1360:      V(1,J)=SMALL
1361:      H(1,J)=SMALL
1362:      CONTINUE
1363:      V(HI,J)=SMALL
1364:      H(HI,J)=SMALL
1365:      CONTINUE
1366:      U(1,NJ)=SMALL
1367:      V(1,NJ)=SMALL
1368:      F(1,NJ)=SMALL
1369:      ED(1,NJ)=SMALL
1370:      IF (IABN.NE.O) GO TO 71
1371:      IF (IABJ.NE.IWALN(I))
1372:      H(1,NJ)=CPL*TWALN(I)
1373:      CONTINUE
1374:      IF (IABN.NE.O) GO TO 74
1375:      DO 72 J=2,NJ
1376:      U(1,J)=F(JOZLE/2) 72
1377:      V(1,J)=F(WALN(I))
1378:      H(1,J)=CPL*TWALN(I)
1379:      CONTINUE
1380: 72 CONTINUE
1381: 74 CONTINUE
1382:
1383:
1384:
1385:
1386:
1387:
1388:
1389:
1390:
1391:
1392:
1393:
1394:
1395:
1396:
1397:
1398:
1399:
1400:
1401:
1402:
1403:
1404:
1405:
1406:
1407:
1408:
1409:
1410:
1411:
1412:
1413:
1414:
1415:
1416:
1417:
1418:
1419:
1420:
1421:
1422:
1423:
1424:
1425:
1426:
1427:
1428:
1429:
1430:
1431:
1432:
1433:
1434:
1435:
1436:
1437:
1438:
1439:
1440:
1441:
1442:
1443:
1444:
1445:
1446:
1447:
1448:
1449:
1450:
1451:
1452:
1453:
1454:
1455:
1456:
1457:
1458:
1459:
1460:
1461:
1462:
1463:
1464:
1465:
1466:
1467:
1468:
1469:
1470:
1471:
1472:
1473:
1474:
1475:
1476:
1477:
1478:
1479:
1480:
1481:
1482:
1483:
1484:
1485:
1486:
1487:
1488:
1489:
1490:
1491:
1492:
1493:
1494:
1495:
1496:
1497:
1498:
1499:
1500:
1501:
1502:
1503:
1504:
1505:
1506:
1507:
1508:
1509:
1510:
1511:
1512:
1513:
1514:
1515:
1516:
1517:
1518:
1519:
1520:
1521:
1522:
1523:
1524:
1525:
1526:
1527:
1528:
1529:
1530:
1531:
1532:
1533:
1534:
1535:
1536:
1537:
1538:
1539:
1540:
1541:
1542:
1543:
1544:
1545:
1546:
1547:
1548:
1549:
1550:
1551:
1552:
1553:
1554:
1555:
1556:
1557:
1558:
1559:
1560:
1561:
1562:
1563:
1564:
1565:
1566:
1567:
1568:
1569:
1570:
1571:
1572:
1573:
1574:
1575:
1576:
1577:
1578:
1579:
1580:
1581:
1582:
1583:
1584:
1585:
1586:
1587:
1588:
1589:
1590:
1591:
1592:
1593:
1594:
1595:
1596:
1597:
1598:
1599:
1600:
1601:
1602:
1603:
1604:
1605:
1606:
1607:
1608:
1609:
1610:
1611:
1612:
1613:
1614:
1615:
1616:
1617:
1618:
1619:
1620:
1621:
1622:
1623:
1624:
1625:
1626:
1627:
1628:
1629:
1630:
1631:
1632:
1633:
1634:
1635:
1636:
1637:
1638:
1639:
1640:
1641:
1642:
1643:
1644:
1645:
1646:
1647:
1648:
1649:
1650:
1651:
1652:
1653:
1654:
1655:
1656:
1657:
1658:
1659:
1660:
1661:
1662:
1663:
1664:
1665:
1666:
1667:
1668:
1669:
1670:
1671:
1672:
1673:
1674:
1675:
1676:
1677:
1678:
1679:
1680:
1681:
1682:
1683:
1684:
1685:
1686:
1687:
1688:
1689:
1690:
1691:
1692:
1693:
1694:
1695:
1696:
1697:
1698:
1699:
1700:
1701:
1702:
1703:
1704:
1705:
1706:
1707:
1708:
1709:
1710:
1711:
1712:
1713:
1714:
1715:
1716:
1717:
1718:
1719:
1720:
1721:
1722:
1723:
1724:
1725:
1726:
1727:
1728:
1729:
1730:
1731:
1732:
1733:
1734:
1735:
1736:
1737:
1738:
1739:
1740:
1741:
1742:
1743:
1744:
1745:
1746:
1747:
1748:
1749:
1750:
1751:
1752:
1753:
1754:
1755:
1756:
1757:
1758:
1759:
1760:
1761:
1762:
1763:
1764:
1765:
1766:
1767:
1768:
1769:
1770:
1771:
1772:
1773:
1774:
1775:
1776:
1777:
1778:
1779:
1780:
1781:
1782:
1783:
1784:
1785:
1786:
1787:
1788:
1789:
1790:
1791:
1792:
1793:
1794:
1795:
1796:
1797:
1798:
1799:
1800:
1801:
1802:
1803:
1804:
1805:
1806:
1807:
1808:
1809:
1810:
1811:
1812:
1813:
1814:
1815:
1816:
1817:
1818:
1819:
1820:
1821:
1822:
1823:
1824:
1825:
1826:
1827:
1828:
1829:
1830:
1831:
1832:
1833:
1834:
1835:
1836:
1837:
1838:
1839:
1840:
1841:
1842:
1843:
1844:
1845:
1846:
1847:
1848:
1849:
1850:
1851:
1852:
1853:
1854:
1855:
1856:
1857:
1858:
1859:
1860:
1861:
1862:
1863:
1864:
1865:
1866:
1867:
1868:
1869:
1870:
1871:
1872:
1873:
1874:
1875:
1876:
1877:
1878:
1879:
1880:
1881:
1882:
1883:
1884:
1885:
1886:
1887:
1888:
1889:
1890:
1891:
1892:
1893:
1894:
1895:
1896:
1897:
1898:
1899:
1900:
1901:
1902:
1903:
1904:
1905:
1906:
1907:
1908:
1909:
1910:
1911:
1912:
1913:
1914:
1915:
1916:
1917:
1918:
1919:
1920:
1921:
1922:
1923:
1924:
1925:
1926:
1927:
1928:
1929:
1930:
1
```

[illegible]

74/1175 721-G TO AC

[illegible]

NYCJRM MAIN

[illegible]


```

PONGRAM MAIN      74/17  QPT=0 TRACE      FIN 4.0+52H      05/13/81  12.05.45
C-----STOP
31C  FORMAT(/11X,10D,*,4X,10X,10V,9X,10M*,9X,10P*,9X,10K,
460  1,9X,10D,*,9X,10H,*,9X,10U,*,9X,10V,*,9X,10W,*,9X,10X,10Y,*)
31I  FORMAT(/6X,13.2X,1P7E10.1,1/13X,1P7E10.1)
402  FORMAT(/25X,11H,7X,5HXU(1),6X,10HS,5,5,COEFF.)
403  FORMAT(/25X,15.51PE11.31)
406  FORMAT(/114X,3HNO,10X,1HX/4,14X,9HHEAT FLUX,6X
465  1,10HHEAT TRANSFER COEFF,
17X,14HNUSSOLI NUMBER,7X,12HFORM. NU.NO.)
405  FORMAT(/15X,12.5110X,1E12.31)
410  FORMAT(/114X,3HNO,10X,1HX/4,14X,9HHEAT FLUX,6X
412  FORMAT(/15X,12.5110X,1E12.41)
      END

```



```

102 DYNP(J)=Y(J+1)-Y(J)
   DYPSP(J)=DYNP(J)
   SEW(J)=0.0
   DO 103 I=2,NIMI
103   SW(I)=0.5*(OYEP(I)+OXPW(I))
   SHS(J)=0.0
   DO 104 J=2,NIMI
104   SN(J)=0.5*(OYNP(J)+OYPS(J))
   DO 105 I=2,N1
105   XU(I)=0.5*(XI(I)+X(I-1))
   OXPWU(I)=0.0
   OXPMU(I)=0.0
   OXEPMU(I)=0.0
   OXEPMU(I)=0.0
   DO 106 I=2,NIMI
106   OXPWU(I)=XU(I+1)-XU(I)
   OXPMU(I)=0.0
   DO 107 I=2,N1
107   SEMU(I)=X(I)-V(I-1)
   SEMU(I)=X(I)
   SEMU(NIMI)=XU(NI)-X(NIMI-1)
   YV(I)=0.0
   PV(I)=0.0
   DO 108 J=2,NJ
108   V(J)=0.5*(RI(J)+RI(J-1))
   YV(J)=0.5*(Y(J)+Y(J-1))
   RCV(J)=0.5*(RV(J)+RV(J+1))
705 CONTINUE
   DYPSPV(I)=0.0
   DYPSPV(I)=0.0
   DYNP(VI)=0.0
   DO 109 J=2,NJ+1
109   DYNPVI(J)=DYNP(V(J))
   SHSPV(I)=0.0
   DO 110 J=2,NJ
110   SHSPV(J)=YV(J)-Y(I-1)
   SHSPV(NJ)=YV(NI)-Y(NJ+1-1)
C
   CALCULATE U-V-LICITIES WEIGHTING FACTORS.....
   DC 303 I=3,NIMI
1005   WFM(I)=SEMU(I-1)/SEMU(I)+SEMU(I)
   WFE(I)=SEW(I+1)/SEW(I+1)+SEW(I)
   CONTINUE
303   PFE(I)=0.0
   PFE(I)=0.0
   CALCULATE V-W-LICITIES WEIGHTING FACTORS.....
   DO 403 J=2,NJ
110   VWS(J)=SHSPV(J-1)/(SHSPV(J-1)+SHSPV(J))
   VWK(J)=SHSV(J-1)/(SHSV(J-1)+SHSV(J))
403 CONTINUE

```



```

SUBROUTINE PRUPS      74/175  30T=0 TRACE      05/13/A1  12.05.65
60  DO 202 J=2,NJM1
    DEN(J)=DEN(J)+CMU/(1+J)
202 CONTINUE
65  DO 100 I=2,NJM1
    DO 102 J=2,NJM1
    VIS(I,J)=E0*0.1 GOTO 102
    IF (DEN(I,J)-E0*0.1) 101,103,104
    VIS(I,J)=DEN(I,J)+2*CMU/(E0(I,J)+VIS(I,J))
102 VIS(I,J)=VIS(I,J)+VIS(I,J)*VIS(I,J)
C-----UNDER RELAXATION
101 VIS(I,J)=CMU*(VIS(I,J)+(1.-URFVIS)*VIS(I,J))
    VIS(I,J)=VIS(I,J)+VIS(I,J)*VIS(I,J)
    IF (DEN(I,J)-E0*0.1) 101,103,104
100 CONTINUE
    RETURN
END

```

```

PRUPS 20
PRUPS 21
PRUPS 22
PRUPS 23
PRUPS 24
PRUPS 25
PRUPS 26
PRUPS 27
PRUPS 28
PRUPS 29
PRUPS 30
PRUPS 31
PRUPS 32
PRUPS 33
PRUPS 34
PRUPS 35
PRUPS 36
PRUPS 37
PRUPS 38
PRUPS 39
PRUPS 40
PRUPS 41
PRUPS 42

```

SUBROUTINE	CALCU	74/175	QIT=0 TRACE	FTN 4.8+529	05/18/81	12.05.45
1						
2						
3						
4						
5						
6						
7						
8						
9						
10						
11						
12						
13						
14						
15						
16						
17						
18						
19						
20						
21						
22						
23						
24						
25						
26						
27						
28						
29						
30						
31						
32						
33						
34						
35						
36						
37						
38						
39						
40						
41						
42						
43						
44						
45						
46						
47						
48						
49						
50						
51						
52						
53						
54						
55						
56						
57						
58						
59						
60						
61						
62						
63						
64						
65						
66						
67						
68						
69						
70						
71						
72						
73						
74						
75						
76						
77						
78						
79						
80						
81						
82						
83						
84						
85						
86						
87						
88						
89						
90						
91						
92						
93						
94						
95						
96						
97						
98						
99						
100						


```

SUBROUTINE CALCU      74/175  021=0 TRACE      05/18/81  12.05.44
110  C-----UNDEP-RELAXATION
      AP(1:J)=AP(1:J)/UPFU
      SU(1:J)=SU(1:J)+AP(1:J)*U(1:J)
      DU(1:J)=DU(1:J)+UPFU
      301 CONTINUE
      300 CONTINUE
      C CHAPTER 4 4 4 SOLUTION OF DIFFERENCE EQUATION 4 4 4 4 4
      C
      ON 400 N=1+NSMPU
      400 CALL LISULV(3,2,0)
      RETURN
      END
      CALCU      77
      CALCU      78
      CALCU      79
      CALCU      80
      CALCU      81
      CALCU      82
      CALCU      83
      CALCU      84
      CALCU      85
      CALCU      86
      CALCU      87
      CALCU      88
      CALCU      89

```

SUBROUTINE CALCV	74/175	74T=0	SPACE	FTN	4.3+52H	05/10/75	12.04.66
1	CHAPTER	0	0	0	0	0	0
5	DIMENSION	U(32,22),V(32,22),W(32,22),P(32,22),PP(32,22),					
10	1,1	EN(32,22),H(32,22),I(32,22),J(32,22),K(32,22),L(32,22),					
15	2,2	SP(32,22),AN(32,22),AS(32,22),AE(32,22),AW(32,22),					
20	3,3	GA(32,22),GE(32,22),GR(32,22),GS(32,22),GT(32,22),					
25	4,4	HA(32,22),HE(32,22),HO(32,22),HU(32,22),HY(32,22),					
30	5,5	IA(32,22),IE(32,22),IO(32,22),IU(32,22),IV(32,22),					
35	6,6	JA(32,22),JE(32,22),JO(32,22),JU(32,22),JV(32,22),					
40	7,7	KA(32,22),KE(32,22),KO(32,22),KU(32,22),KV(32,22),					
45	8,8	LA(32,22),LE(32,22),LO(32,22),LU(32,22),LV(32,22),					
50	9,9	MA(32,22),ME(32,22),MO(32,22),MU(32,22),MV(32,22),					
55	10,10	NA(32,22),NE(32,22),NO(32,22),NU(32,22),NV(32,22),					
	11,11	OA(32,22),OE(32,22),OO(32,22),OU(32,22),OV(32,22),					
	12,12	PA(32,22),PE(32,22),PO(32,22),PU(32,22),PV(32,22),					
	13,13	QA(32,22),QE(32,22),QO(32,22),QU(32,22),QV(32,22),					
	14,14	RA(32,22),RE(32,22),RO(32,22),RU(32,22),RV(32,22),					
	15,15	SA(32,22),SE(32,22),SO(32,22),SU(32,22),SV(32,22),					
	16,16	TA(32,22),TE(32,22),TO(32,22),TU(32,22),TV(32,22),					
	17,17	UA(32,22),UE(32,22),UO(32,22),UU(32,22),UV(32,22),					
	18,18	VA(32,22),VE(32,22),VO(32,22),VU(32,22),VV(32,22),					
	19,19	WA(32,22),WE(32,22),WO(32,22),WU(32,22),WV(32,22),					
	20,20	XA(32,22),XE(32,22),XO(32,22),XU(32,22),XV(32,22),					
	21,21	YA(32,22),YE(32,22),YO(32,22),YU(32,22),YV(32,22),					
	22,22	ZA(32,22),ZE(32,22),ZO(32,22),ZU(32,22),ZV(32,22),					
	23,23	AA(32,22),EA(32,22),OA(32,22),UA(32,22),VA(32,22),					
	24,24	BA(32,22),BE(32,22),BO(32,22),BU(32,22),BV(32,22),					
	25,25	CA(32,22),CE(32,22),CO(32,22),CU(32,22),CV(32,22),					
	26,26	DA(32,22),DE(32,22),DO(32,22),DU(32,22),DV(32,22),					
	27,27	EA(32,22),EE(32,22),EO(32,22),EU(32,22),EV(32,22),					
	28,28	FA(32,22),FE(32,22),FO(32,22),FU(32,22),FV(32,22),					
	29,29	GA(32,22),GE(32,22),GO(32,22),GU(32,22),GV(32,22),					
	30,30	HA(32,22),HE(32,22),HO(32,22),HU(32,22),HV(32,22),					
	31,31	IA(32,22),IE(32,22),IO(32,22),IU(32,22),IV(32,22),					
	32,32	JA(32,22),JE(32,22),JO(32,22),JU(32,22),JV(32,22),					
	33,33	KA(32,22),KE(32,22),KO(32,22),KU(32,22),KV(32,22),					
	34,34	LA(32,22),LE(32,22),LO(32,22),LU(32,22),LV(32,22),					
	35,35	MA(32,22),ME(32,22),MO(32,22),MU(32,22),MV(32,22),					
	36,36	NA(32,22),NE(32,22),NO(32,22),NU(32,22),NV(32,22),					
	37,37	OA(32,22),OE(32,22),OO(32,22),OU(32,22),OV(32,22),					
	38,38	PA(32,22),PE(32,22),PO(32,22),PU(32,22),PV(32,22),					
	39,39	QA(32,22),QE(32,22),QO(32,22),QU(32,22),QV(32,22),					
	40,40	RA(32,22),RE(32,22),RO(32,22),RU(32,22),RV(32,22),					
	41,41	SA(32,22),SE(32,22),SO(32,22),SU(32,22),SV(32,22),					
	42,42	TA(32,22),TE(32,22),TO(32,22),TU(32,22),TV(32,22),					
	43,43	UA(32,22),UE(32,22),UO(32,22),UU(32,22),UV(32,22),					
	44,44	VA(32,22),VE(32,22),VO(32,22),VU(32,22),VV(32,22),					
	45,45	WA(32,22),WE(32,22),WO(32,22),WU(32,22),WV(32,22),					
	46,46	XA(32,22),XE(32,22),XO(32,22),XU(32,22),XV(32,22),					
	47,47	YA(32,22),YE(32,22),YO(32,22),YU(32,22),YV(32,22),					
	48,48	ZA(32,22),ZE(32,22),ZO(32,22),ZU(32,22),ZV(32,22),					
	49,49	AA(32,22),EA(32,22),OA(32,22),UA(32,22),VA(32,22),					
	50,50	BA(32,22),BE(32,22),BO(32,22),BU(32,22),BV(32,22),					
	51,51	CA(32,22),CE(32,22),CO(32,22),CU(32,22),CV(32,22),					
	52,52	DA(32,22),DE(32,22),DO(32,22),DU(32,22),DV(32,22),					
	53,53	EA(32,22),EE(32,22),EO(32,22),EU(32,22),EV(32,22),					
	54,54	FA(32,22),FE(32,22),FO(32,22),FU(32,22),FV(32,22),					
	55,55	GA(32,22),GE(32,22),GO(32,22),GU(32,22),GV(32,22),					
	56,56	HA(32,22),HE(32,22),HO(32,22),HU(32,22),HV(32,22),					
	57,57	IA(32,22),IE(32,22),IO(32,22),IU(32,22),IV(32,22),					
	58,58	JA(32,22),JE(32,22),JO(32,22),JU(32,22),JV(32,22),					
	59,59	KA(32,22),KE(32,22),KO(32,22),KU(32,22),KV(32,22),					
	60,60	LA(32,22),LE(32,22),LO(32,22),LU(32,22),LV(32,22),					
	61,61	MA(32,22),ME(32,22),MO(32,22),MU(32,22),MV(32,22),					
	62,62	NA(32,22),NE(32,22),NO(32,22),NU(32,22),NV(32,22),					
	63,63	OA(32,22),OE(32,22),OO(32,22),OU(32,22),OV(32,22),					
	64,64	PA(32,22),PE(32,22),PO(32,22),PU(32,22),PV(32,22),					
	65,65	QA(32,22),QE(32,22),QO(32,22),QU(32,22),QV(32,22),					
	66,66	RA(32,22),RE(32,22),RO(32,22),RU(32,22),RV(32,22),					
	67,67	SA(32,22),SE(32,22),SO(32,22),SU(32,22),SV(32,22),					
	68,68	TA(32,22),TE(32,22),TO(32,22),TU(32,22),TV(32,22),					
	69,69	UA(32,22),UE(32,22),UO(32,22),UU(32,22),UV(32,22),					
	70,70	VA(32,22),VE(32,22),VO(32,22),VU(32,22),VV(32,22),					
	71,71	WA(32,22),WE(32,22),WO(32,22),WU(32,22),WV(32,22),					
	72,72	XA(32,22),XE(32,22),XO(32,22),XU(32,22),XV(32,22),					
	73,73	YA(32,22),YE(32,22),YO(32,22),YU(32,22),YV(32,22),					
	74,74	ZA(32,22),ZE(32,22),ZO(32,22),ZU(32,22),ZV(32,22),					
	75,75	AA(32,22),EA(32,22),OA(32,22),UA(32,22),VA(32,22),					
	76,76	BA(32,22),BE(32,22),BO(32,22),BU(32,22),BV(32,22),					
	77,77	CA(32,22),CE(32,22),CO(32,22),CU(32,22),CV(32,22),					
	78,78	DA(32,22),DE(32,22),DO(32,22),DU(32,22),DV(32,22),					
	79,79	EA(32,22),EE(32,22),EO(32,22),EU(32,22),EV(32,22),					
	80,80	FA(32,22),FE(32,22),FO(32,22),FU(32,22),FV(32,22),					
	81,81	GA(32,22),GE(32,22),GO(32,22),GU(32,22),GV(32,22),					
	82,82	HA(32,22),HE(32,22),HO(32,22),HU(32,22),HV(32,22),					
	83,83	IA(32,22),IE(32,22),IO(32,22),IU(32,22),IV(32,22),					
	84,84	JA(32,22),JE(32,22),JO(32,22),JU(32,22),JV(32,22),					
	85,85	KA(32,22),KE(32,22),KO(32,22),KU(32,22),KV(32,22),					
	86,86	LA(32,22),LE(32,22),LO(32,22),LU(32,22),LV(32,22),					
	87,87	MA(32,22),ME(32,22),MO(32,22),MU(32,22),MV(32,22),					
	88,88	NA(32,22),NE(32,22),NO(32,22),NU(32,22),NV(32,22),					
	89,89	OA(32,22),OE(32,22),OO(32,22),OU(32,22),OV(32,22),					
	90,90	PA(32,22),PE(32,22),PO(32,22),PU(32,22),PV(32,22),					
	91,91	QA(32,22),QE(32,22),QO(32,22),QU(32,22),QV(32,22),					
	92,92	RA(32,22),RE(32,22),RO(32,22),RU(32,22),RV(32,22),					
	93,93	SA(32,22),SE(32,22),SO(32,22),SU(32,22),SV(32,22),					
	94,94	TA(32,22),TE(32,22),TO(32,22),TU(32,22),TV(32,22),					
	95,95	UA(32,22),UE(32,22),UO(32,22),UU(32,22),UV(32,22),					
	96,96	VA(32,22),VE(32,22),VO(32,22),VU(32,22),VV(32,22),					
	97,97	WA(32,22),WE(32,22),WO(32,22),WU(32,22),WV(32,22),					
	98,98	XA(32,22),XE(32,22),XO(32,22),XU(32,22),XV(32,22),					
	99,99	YA(32,22),YE(32,22),YO(32,22),YU(32,22),YV(32,22),					
	100,100	ZA(32,22),ZE(32,22),ZO(32,22),ZU(32,22),ZV(32,22),					

[illegible]

[illegible]

```

SUBROUTINE CALCP      74/175  OPT=0 TRACE      05/18/81  12.05.45
FTN 4.0+528
115  C CHAPTER 5 5 5 CORRECT VELOCITIES AND PRESSURE 5 5 5 5
      DO 400 N=1,NSMPP
      400 CALL LISOLV(2,2,PP1)
120  C-----VELOCITIES
      DO 500 J=2,NJM1
      500 J=2,NJM1
      IF (J.NE.2) V(1,J)=V(1,J)+8*V(1,J)+16*V(1,J)-8*V(1,J)
125  301 CONTINUE
      C-----PRESSURES (WITH PROVISION FOR UNDER-RELAXATION)
      PPREF=PP(1,PPREF)
      DO 502 I=2,NJM1
      502 I=2,NJM1
      P(1,I)=8*PP(1,I)+URFP*(PP(1,I)-PPREF)
130  302 CONTINUE
      302 CONTINUE
      END
135

```

```

77  CALCP
78  CALCP
79  CALCP
80  CALCP
81  CALCP
82  CALCP
83  CALCP
84  CALCP
85  CALCP
86  CALCP
87  CALCP
88  CALCP
89  CALCP
90  CALCP
91  CALCP
92  CALCP
93  CALCP
94  CALCP
95  CALCP
96  CALCP
97  CALCP

```



```

SUBROUTINE CALCIE      74/174      OPT=0 TRACE      05/18/81      12.05.44
11> C CHAPTER 2 2 2 2 2 2 PROBLEM MODIFICATIONS 2 2 2 2 2 2
C CALL MODEL
C CHAPTER 3 FINAL COEFFICIENT ASSEMBLY AND RESIDUAL SOURCE CALCULATION 3
C
      NLSOPK=0.0
      DO 300 I=2,NINI
      DO 301 J=2,NJN1
      AP(I,J)=AN(I,J)+AS(I,J)*AC(I,J)+AW(I,J)-SP(I,J)
      PLSOR=AN(I,J)+AS(I,J)*TE(I,J)-1)+AE(I,J)+TE(I+1,J)
      1 VOL=K(J)*SEW(I)*SNS(I)
      SURVOL=GRAT*VOL
      IF (SP(I,J).GT.0) 5*SURVOL
      RLSOR=RESOR+RARS*TRFSOR
      C-----UNDER-RELAXATION
      AP(I,J)=AP(I,J)/(1.-URFK)+AP(I,J)+TE(I,J)
      301 CONTINUE
      300 CONTINUE
C CHAPTER 4 4 4 4 4 SOLUTION OF DIFFERENCE EQUATIONS 4 4 4 4 4
C
      DO 400 N=1,NLSOPK
      400 CALL LISOLV(2,P,TE)
      RETURN
      END

```

```

77 CALCIE
78 CALCIE
79 CALCIE
80 CALCIE
81 CALCIE
82 CALCIE
83 CALCIE
84 CALCIE
85 CALCIE
86 CALCIE
87 CALCIE
88 CALCIE
89 CALCIE
90 CALCIE
91 CALCIE
92 CALCIE
93 CALCIE
94 CALCIE
95 CALCIE
96 CALCIE
97 CALCIE
98 CALCIE
99 CALCIE
100 CALCIE
101 CALCIE
102 CALCIE
103 CALCIE
104 CALCIE

```

1	2	3	4	5	6	7	8	9	10	11	12	13	14	15	16	17	18	19	20	21	22	23	24	25	26	27	28	29	30	31	32	33	34	35	36	37	38	39	40	41	42	43	44	45	46	47	48	49	50	51	52	53	54	55	56	57	58	59	60	61	62	63	64	65	66	67	68	69	70	71	72	73	74	75	76	77	78	79	80	81	82	83	84	85	86	87	88	89	90	91	92	93	94	95	96	97	98	99	100
1	2	3	4	5	6	7	8	9	10	11	12	13	14	15	16	17	18	19	20	21	22	23	24	25	26	27	28	29	30	31	32	33	34	35	36	37	38	39	40	41	42	43	44	45	46	47	48	49	50	51	52	53	54	55	56	57	58	59	60	61	62	63	64	65	66	67	68	69	70	71	72	73	74	75	76	77	78	79	80	81	82	83	84	85	86	87	88	89	90	91	92	93	94	95	96	97	98	99	100
1	2	3	4	5	6	7	8	9	10	11	12	13	14	15	16	17	18	19	20	21	22	23	24	25	26	27	28	29	30	31	32	33	34	35	36	37	38	39	40	41	42	43	44	45	46	47	48	49	50	51	52	53	54	55	56	57	58	59	60	61	62	63	64	65	66	67	68	69	70	71	72	73	74	75	76	77	78	79	80	81	82	83	84	85	86	87	88	89	90	91	92	93	94	95	96	97	98	99	100
1	2	3	4	5	6	7	8	9	10	11	12	13	14	15	16	17	18	19	20	21	22	23	24	25	26	27	28	29	30	31	32	33	34	35	36	37	38	39	40	41	42	43	44	45	46	47	48	49	50	51	52	53	54	55	56	57	58	59	60	61	62	63	64	65	66	67	68	69	70	71	72	73	74	75	76	77	78	79	80	81	82	83	84	85	86	87	88	89	90	91	92	93	94	95	96	97	98	99	100
1	2	3	4	5	6	7	8	9	10	11	12	13	14	15	16	17	18	19	20	21	22	23	24	25	26	27	28	29	30	31	32	33	34	35	36	37	38	39	40	41	42	43	44	45	46	47	48	49	50	51	52	53	54	55	56	57	58	59	60	61	62	63	64	65	66	67	68	69	70	71	72	73	74	75	76	77	78	79	80	81	82	83	84	85	86	87	88	89	90	91	92	93	94	95	96	97	98	99	100
1	2	3	4	5	6	7	8	9	10	11	1																																																																																								

[illegible]


```

SPURDTYPE CALCH      74/175      DT=0 TRACE      FIN 4.8+528      05/19/81      12.05.45
201
202
203
204
205
206
207
208
209
210
211
212
213
214
215
216
217
218
219
220
221
222
223
224
225
226
227
228
229
230
231
232
233
234
235
236
237
238
239
240
241
242
243
244
245
246
247
248
249
250
251
252
253
254
255
256
257
258
259
260
261
262
263
264
265
266
267
268
269
270
271
272
273
274
275
276
277
278
279
280
281
282
283
284
285
286
287
288
289
290
291
292
293
294
295
296
297
298
299
300
301
302
303
304
305
306
307
308
309
310
311
312
313
314
315
316
317
318
319
320
321
322
323
324
325
326
327
328
329
330
331
332
333
334
335
336
337
338
339
340
341
342
343
344
345
346
347
348
349
350
351
352
353
354
355
356
357
358
359
360
361
362
363
364
365
366
367
368
369
370
371
372
373
374
375
376
377
378
379
380
381
382
383
384
385
386
387
388
389
390
391
392
393
394
395
396
397
398
399
400
401
402
403
404
405
406
407
408
409
410
411
412
413
414
415
416
417
418
419
420
421
422
423
424
425
426
427
428
429
430
431
432
433
434
435
436
437
438
439
440
441
442
443
444
445
446
447
448
449
450
451
452
453
454
455
456
457
458
459
460
461
462
463
464
465
466
467
468
469
470
471
472
473
474
475
476
477
478
479
480
481
482
483
484
485
486
487
488
489
490
491
492
493
494
495
496
497
498
499
500
501
502
503
504
505
506
507
508
509
510
511
512
513
514
515
516
517
518
519
520
521
522
523
524
525
526
527
528
529
530
531
532
533
534
535
536
537
538
539
540
541
542
543
544
545
546
547
548
549
550
551
552
553
554
555
556
557
558
559
560
561
562
563
564
565
566
567
568
569
570
571
572
573
574
575
576
577
578
579
580
581
582
583
584
585
586
587
588
589
590
591
592
593
594
595
596
597
598
599
600
601
602
603
604
605
606
607
608
609
610
611
612
613
614
615
616
617
618
619
620
621
622
623
624
625
626
627
628
629
630
631
632
633
634
635
636
637
638
639
640
641
642
643
644
645
646
647
648
649
650
651
652
653
654
655
656
657
658
659
660
661
662
663
664
665
666
667
668
669
670
671
672
673
674
675
676
677
678
679
680
681
682
683
684
685
686
687
688
689
690
691
692
693
694
695
696
697
698
699
700
701
702
703
704
705
706
707
708
709
710
711
712
713
714
715
716
717
718
719
720
721
722
723
724
725
726
727
728
729
730
731
732
733
734
735
736
737
738
739
740
741
742
743
744
745
746
747
748
749
750
751
752
753
754
755
756
757
758
759
760
761
762
763
764
765
766
767
768
769
770
771
772
773
774
775
776
777
778
779
780
781
782
783
784
785
786
787
788
789
790
791
792
793
794
795
796
797
798
799
800
801
802
803
804
805
806
807
808
809
810
811
812
813
814
815
816
817
818
819
820
821
822
823
824
825
826
827
828
829
830
831
832
833
834
835
836
837
838
839
840
841
842
843
844
845
846
847
848
849
850
851
852
853
854
855
856
857
858
859
860
861
862
863
864
865
866
867
868
869
870
871
872
873
874
875
876
877
878
879
880
881
882
883
884
885
886
887
888
889
890
891
892
893
894
895
896
897
898
899
900
901
902
903
904
905
906
907
908
909
910
911
912
913
914
915
916
917
918
919
920
921
922
923
924
925
926
927
928
929
930
931
932
933
934
935
936
937
938
939
940
941
942
943
944
945
946
947
948
949
950
951
952
953
954
955
956
957
958
959
960
961
962
963
964
965
966
967
968
969
970
971
972
973
974
975
976
977
978
979
980
981
982
983
984
985
986
987
988
989
990
991
992
993
994
995
996
997
998
999
1000

```

115 SUBROUTINE CALCH 74/175 OPT=0 TRACE 05/18/81 12.05.46
 RETURN
 END
 CALCH 77
 CALCH 78

[illegible]

[illegible]

[illegible]

```

COMPUTING PRIMUM      74/L7      121=0 TRACE      12.05.4*
175      IF (YPLUSA,LE,11.63) GO TO 1801
          TMULT = DENM*CDTERH+SQRK+CAPPA/ALOG(ELDG*YPLUSA)
          GL TO 1815
          TMULT = VISCOS/YP
1801      CONTINUE
1815      SF(I,J)=SP(I,J)-TMULT*SEW(I)*RV(NJ)
1800      AN(I,J)=0.0
          SIDE WALL
          CDTERH = CMU*0.75
          XP = X(STEP)-YU(I,STEP)
          DO 1802 I=2,NM1
            IF (I,LT,JNDLE) GO TO 1802
            SQRK = SQRTE(I,J)
            DENM = DEN(I,J)
            YPLUSA = YPLUSA(I,J)
            IF (XPLUSA,LE,11.63) GO TO 1803
            TMULT = DENM*CDTERH+SQRK+CAPPA/ALOG(ELDG*YPLUSA)
            GL TO 1816
            TMULT = VISCOS/XP
1803      CONTINUE
1816      SP(I,J)=SP(I,J)-TMULT*SNS(J)*R(J)
1802      CONTINUE
          SYMMETRY AXIS
          DO 1804 I=2,NM1
            AS(I,2)=G.0
            OUTLT
          I=NMI
          ON 405 J=2,NJM1
            AREA = A(I)+SNS(I)
            CM4 = DEN(I,1)*U(2,1)*AREA
            DM4 = VIS(I,1)*AREF(IXPM(2)
            AM(2,J)=AMX1(ARS(.5*CM4),DM4)+.5*CM4
            IF (J,GT,JNDLE) AM(2,J)=0.0
            IF (J,GT,JNDLE) AM(2,J)=0.0
            CONTINUE
            P. TURN
          405      CONTINUE
          CHAPTER 6 6 6 6 6 TURBULENT KINETIC ENERGY
          ENTRY MUDIE
          TUP WALL
          DO 9 J=2,NJ1
            J=NJM1
            YP = 0.2*G(I,J)+U(I+1,J)
            YP = DYPSEN(I)
            YC = SNS(I)
            VC = 0.2*G(I,1-1)+U(I+1,J-1)
            VC = 0.2*G(I,VP+VS)
            VC = X(2)*VC+2*(M(I,J-1)*2)
            VC = X(2)*VC+2*(M(I,J)*2)
            VC = SQRTE(I,J)+V(I,J+1)/PRTE
            GAMM=0.2*(V(I,J)+V(I,J+1))/PRTE
            VISM = GAMM
            VISM = RCV(J)*SNS(J)*SEW(I)
            SU(I,J)=VISM*VC+VUL/(YP+YC)+SU(I,J)
            IF (VP,LE,1.5-10) VP=1.5-10
            SP(I,J)=-(DEN(I,J))**2*CMU*TE(I,J)*VC*YP/(YC*VP*VISM)*VUL+SP(I,J)
            AN(I,J)=0.0

```



```

SUBROUTINE PROMOD      74.7.75  0210 TRACE      FFN 4.0+20      05/19/81  17.05.45
C-----
ENTRY MODT=1
TOP CALL
CDTERM=CMU*0.25
VI=V(INJ)-V(INJ1)
J=NJNL
DO CLC 1=2,NJ1
  DENUS=DENI(1)
  SORTR=SORTR(F(I,J))
  VOL=AC(J)+SNS(J)+SEM(I)
  YPLUSN(I)=JFNU+SORTR*CDTERM*YP/VISCOS
  YPLUSA=YPLUSN(I)
  IF(YPLUSA.LE.11.63) GO TO 809
  TMULTW(I)=DENUS*CDTERM*PSORTK*CAPP/ALOG(ELUG*YPLUSA)
  GO TO 808
809
  TMULTW(I)=VIS(I,J)/YP
  TAURUT(I)=TMULTW(I)*.5*(U(I,J)+U(I+1,J))
  TAUN(I)=TAURUT(I)
  GENC0=ABS(TAUN(I))*2.5*(U(I,J)+U(I+1,J))/YP
  DUDY=(U(I,J)+U(I+1,J))/2*(U(I,J)+U(I+1,J))+SNS(J)
  101 J=J+1+U(I+1,J)/SNS(I)
  GENPES=GEN(I,J)-VIS(I,J)+DUDY**2
  IF(ASHO.EQ.0)GO TO 515
  TAUN(I)=TMULTW(I)*W(I,J)
  GENC0=GENC0+ABS(TAUN(I))*2*(U(I,J)+U(I+1,J))/YP-ABS(TAUN(I))*W(I,J)/R(J)
  DUDY=(U(I,J)+U(I+1,J))/2*(U(I,J)+U(I+1,J))+SNS(J)
  W(I)=W(I)+J/2*J
  GENPES=GENPES-VIS(I,J)+DUDY*WDR**2
  TAUN(I)=SORT(TAURUT(I)+2*TAUN(I))+2
  515 CONTINUE
  GEN(I,J)=GENPES*GENC0
  611 CONTINUE
  D1TERM=DEMI(I)*(CMJ**75)*SORTR*YPLUSN(I)/YP
  D1TERM=DEMI(I)*LE(I,63) GO TO 811
  GO TO 612
  612 CONTINUE
  SP(I,J)=GEN(I,J)+VOL+SUKD(I,J)
  SP(I,J)=D1TERM*VOL+SUKD(I,J)
  610 AN(I,J)=G.J
C-----
XP=XTSTEP)-XU(ISTEP)
1=151P
DO 620 J=INQZL,NJ1
  DENV=DENI(J)
  SORTR=SORTR(F(I,J))
  VOL=AC(J)+SNS(J)+SEM(I)
  XPLUSN(J)=DENV*SP(I)+CDTERM*XP/VISCOS
  XPLUSA=XPLUSN(J)
  11 XPLUSA.LE.11.63) GO TO 817
  TMULTW(J)=JFNU*CDTERM*SORTR*CAPP/ALOG(ELUG*XPLUSA)
  GO TO 818
  817
  TMULTW(J)=VIS(I,J)/XP
  TAURUT(J)=TMULTW(J)*.5*(V(I,J)+V(I+1,J))
  GENC0=ABS(TAURUT(J))*2.5*(V(I,J)+V(I+1,J))/XP
  DUDY=(V(I,J)+V(I+1,J))/2*(V(I,J)+V(I+1,J))+SNS(I)
  11-1 J=J+1+V(I+1,J)/SNS(I)
  GENPES=GEN(I,J)-VIS(I,J)+DUDY**2
  300 PROMOD 248
  301 PROMOD 249
  302 PROMOD 250
  303 PROMOD 251
  304 PROMOD 252
  305 PROMOD 253
  306 PROMOD 254
  307 PROMOD 255
  308 PROMOD 256
  309 PROMOD 257
  310 PROMOD 258
  311 PROMOD 259
  312 PROMOD 260
  313 PROMOD 261
  314 PROMOD 262
  315 PROMOD 263
  316 PROMOD 264
  317 PROMOD 265
  318 PROMOD 266
  319 PROMOD 267
  320 PROMOD 268
  321 PROMOD 269
  322 PROMOD 270
  323 PROMOD 271
  324 PROMOD 272
  325 PROMOD 273
  326 PROMOD 274
  327 PROMOD 275
  328 PROMOD 276
  329 PROMOD 277
  330 PROMOD 278
  331 PROMOD 279
  332 PROMOD 280
  333 PROMOD 281
  334 PROMOD 282
  335 PROMOD 283
  336 PROMOD 284
  337 PROMOD 285
  338 PROMOD 286
  339 PROMOD 287
  340 PROMOD 288
  341 PROMOD 289
  342 PROMOD 290
  343 PROMOD 291
  344 PROMOD 292
  345 PROMOD 293
  346 PROMOD 294
  347 PROMOD 295
  348 PROMOD 296
  349 PROMOD 297
  350 PROMOD 298
  351 PROMOD 299
  352 PROMOD 300
  353 PROMOD 301
  354 PROMOD 302
  355 PROMOD 303
  356 PROMOD 304

```


	SUBROUTINE	PRGMOD	74/17	DT-3	TPACH	FIN	4.3*528	05/18/81	17.05.65
460								PRGMOD	419
								PRGMOD	420
								PRGMOD	421
								PRGMOD	422
								PRGMOD	423
								PRGMOD	424
								PRGMOD	425
								PRGMOD	426
								PRGMOD	427
								PRGMOD	428
								PRGMOD	429
								PRGMOD	430
								PRGMOD	431
								PRGMOD	432
								PRGMOD	433
								PRGMOD	434
								PRGMOD	435
								PRGMOD	436
								PRGMOD	437
								PRGMOD	438
								PRGMOD	439
								PRGMOD	440
								PRGMOD	441
								PRGMOD	442
								PRGMOD	443
								PRGMOD	444
								PRGMOD	445
								PRGMOD	446
								PRGMOD	447
								PRGMOD	448
								PRGMOD	449
								PRGMOD	450
								PRGMOD	451
								PRGMOD	452
								PRGMOD	453
								PRGMOD	454


```

T(I,J+1)=T(I,J+1)/CPI
TVALN(I)=T(I,J+1)
CONTINUE
171C
1903 TIRM=GAMMA(I)+AREA
      SU(I,J)=SU(I,J)+TERM*(I,J+1)
      SP(I,J)=SP(I,J)-TERM
903 CONTINUE
908 IF(IABN.EQ.0)GO TO 904
      I=2
      DO 1904 J=2,NM1
        IF(IJ.LS.JNDZ)GO TO 1904
        AM(I,J)=C.
        IF(IABN.EQ.1)GO TO 907
        I=2
        DO 905 J=2,NJ1
          AM(I,J)=0.
          AREA=RCJ)+SNS(I)
          GAMMA(I)=VISCIS/PRLAM/KP
          XPLUSA=XPLUSW(I)
          IF(XPLUSA.LE.-11.63)GO TO 1905
          UPLUS=ALOG(FCIG*XPLUSA)/CAPPA
          GAMMA(I)=DEH(I)+CONERN+SOKTITE(I,J))/((PRH*(UPLUS+PFUN))
1905 CONTINUE
      TERM=GAMMA(I)+AREA
      SU(I,J)=SU(I,J)+TERM*(I-L,J)
      SP(I,J)=SP(I,J)-TERM
905 CONTINUE
907 DO 906 I=2,N1
      NI(I)=NI(I,2)
      AS(I,2)=0.
906 CONTINUE
908 END

```


۱۲۳۴۵۶۷۸۹۱۰۱۱۱۲۱۳۱۴۱۵۱۶۱۷۱۸۱۹۲۰۲۱۲۲۲۳۲۴۲۵۲۶۲۷۲۸۲۹۳۰
 ۳۱۳۲۳۳۳۴۳۵۳۶۳۷۳۸۳۹۴۰۴۱۴۲۴۳۴۴۴۵۴۶۴۷۴۸۴۹۵۰
 ۵۱۵۲۵۳۵۴۵۵۵۶۵۷۵۸۵۹۶۰۶۱۶۲۶۳۶۴۶۵۶۶۶۷۶۸۶۹۷۰
 ۷۱۷۲۷۳۷۴۷۵۷۶۷۷۷۸۷۹۸۰۸۱۸۲۸۳۸۴۸۵۸۶۸۷۸۸۸۹۹۰
 ۹۱۹۲۹۳۹۴۹۵۹۶۹۷۹۸۹۹۱۰۰

220 416 531 210 476 543

AD-A108 095

ARIZONA UNIV TUCSON ENGINEERING EXPERIMENT STATION
CONVECTIVE HEAT TRANSFER FOR SHIP PROPULSION.(U)
APR 81 M A HABIB, D M MCLEIGOT

F/G 20/13

UNCLASSIFIED

1248-8

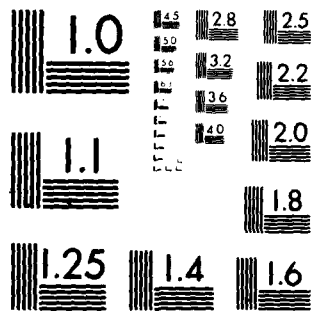
N00014-75-C-0694

NL

2-2
A. G. G. G. G.



END
DATE
FILMED
82
DTIC



MICROCOPY RESOLUTION TEST CHART
NATIONAL BUREAU OF STANDARDS-1963-A

1 X(1) S.S. COEFF.

2	7.428E-02	0.	0.	0.	1.052E+01
3	2.228E-01	0.	0.	0.	1.349E+01
4	3.714E-01	0.	0.	0.	1.930E+01
5	5.943E-01	0.	0.	0.	2.663E+01
6	8.914E-01	0.	0.	0.	3.051E+01
7	1.189E+00	0.	0.	0.	3.658E+01
8	1.634E+00	0.	0.	0.	4.297E+01
9	2.228E+00	0.	0.	0.	5.963E+01
10	2.971E+00	0.	0.	0.	5.497E+01
11	3.863E+00	0.	0.	0.	5.811E+01
12	5.051E+00	0.	0.	0.	7.868E+01
13	6.537E+00	0.	0.	0.	5.627E+01
14	8.320E+00	0.	0.	0.	5.067E+01
15	1.040E+01	0.	0.	0.	6.305E+01
16	1.293E+01	0.	0.	0.	3.584E+01
17	1.590E+01	0.	0.	0.	3.078E+01
18	1.931E+01	0.	0.	0.	2.798E+01
19	2.303E+01	0.	0.	0.	2.653E+01
20	2.748E+01	0.	0.	0.	2.564E+01
21	3.224E+01	0.	0.	0.	2.490E+01
22	3.714E+01	0.	0.	0.	2.415E+01
23	4.308E+01	0.	0.	0.	2.341E+01
24	5.051E+01	0.	0.	0.	2.277E+01
25	5.943E+01	0.	0.	0.	2.230E+01
26	6.834E+01	0.	0.	0.	2.202E+01
27	7.828E+01	0.	0.	0.	2.192E+01

2 0.
3 0.
4 0.
5 0.
6 0.
7 0.
8 0.
9 0.
10 0.
11 0.
12 0.
13 0.
14 0.
15 0.
16 0.
17 0.
18 0.
19 0.
20 0.
21 0.
22 0.
23 0.
24 0.
25 0.
26 0.
27 0.

NO.	X/H	HEAT FLUX	HEAT TRANSFER COEFF.	NUSEFF NUMBER	NORM. NU. NO.
2	.743E+01	.130E+03	.543E+02	.495E+02	.528E+00
3	.223E+00	.178E+03	.690E+02	.630E+02	.670E+00
4	.371E+00	.291E+03	.101E+03	.92E+02	.993E+00
5	.594E+00	.420E+03	.133E+03	.121E+03	.129E+01
6	.891E+00	.579E+03	.169E+03	.154E+03	.164E+01
7	.119E+01	.763E+03	.206E+03	.188E+03	.200E+01
8	.163E+01	.101E+04	.249E+03	.227E+03	.242E+01
9	.223E+01	.130E+04	.294E+03	.268E+03	.286E+01
10	.297E+01	.167E+04	.337E+03	.307E+03	.320E+01
11	.386E+01	.189E+04	.365E+03	.335E+03	.355E+01
12	.505E+01	.192E+04	.379E+03	.345E+03	.368E+01
13	.654E+01	.186E+04	.377E+03	.343E+03	.366E+01
14	.832E+01	.199E+04	.355E+03	.324E+03	.345E+01
15	.104E+02	.178E+04	.317E+03	.288E+03	.308E+01
16	.129E+02	.172E+04	.277E+03	.253E+03	.269E+01
17	.159E+02	.210E+04	.245E+03	.223E+03	.238E+01
18	.193E+02	.242E+04	.223E+03	.203E+03	.217E+01
19	.230E+02	.259E+04	.206E+03	.188E+03	.200E+01
20	.275E+02	.315E+04	.192E+03	.175E+03	.187E+01
21	.322E+02	.330E+04	.178E+03	.162E+03	.173E+01
22	.371E+02	.328E+04	.163E+03	.148E+03	.158E+01
23	.431E+02	.306E+04	.148E+03	.135E+03	.144E+01
24	.509E+02	.287E+04	.137E+03	.125E+03	.133E+01
25	.594E+02	.275E+04	.129E+03	.118E+03	.126E+01
26	.683E+02	.271E+04	.126E+03	.115E+03	.123E+01
27	.743E+02	.277E+04	.126E+03	.115E+03	.122E+01

NO.	IBULK	IDIFF
2	.3097E+03	.2398E+01
3	.3097E+03	.2985E+01
4	.3097E+03	.2873E+01
5	.3097E+03	.3154E+01
6	.3098E+03	.3429E+01
7	.3098E+03	.3704E+01
8	.3098E+03	.4066E+01
9	.3099E+03	.4416E+01
10	.3099E+03	.4953E+01
11	.3100E+03	.5177E+01
12	.3101E+03	.5076E+01
13	.3102E+03	.4951E+01
14	.3104E+03	.5600E+01
15	.3106E+03	.5624E+01
16	.3108E+03	.6210E+01
17	.3110E+03	.8558E+01
18	.3113E+03	.1087E+02
19	.3116E+03	.1255E+02
20	.3120E+03	.1638E+02
21	.3124E+03	.1857E+02
22	.3128E+03	.2016E+02
23	.3133E+03	.2066E+02
24	.3140E+03	.2103E+02
25	.3147E+03	.2127E+02
26	.3155E+03	.2152E+02
27	.3160E+03	.2201E+02
		.3121E+03
		.3123E+03
		.3126E+03
		.3129E+03
		.3132E+03
		.3135E+03
		.3139E+03
		.3143E+03
		.3149E+03
		.3152E+03
		.3152E+03
		.3160E+03
		.3162E+03
		.3170E+03
		.3196E+03
		.3222E+03
		.3242E+03
		.3284E+03
		.3310E+03
		.3330E+03
		.3340E+03
		.3350E+03
		.3360E+03
		.3370E+03
		.3380E+03

REFERENCES

- Beltagui, S. A. and N. R. L. MacCallum, 1976. Aerodynamics of vane-swirled flames in furnaces, J. Inst. Fuel, 49, p. 183.
- Bradshaw, P., 1973. Effects of streamline curvature on turbulent flows, AGARDograph No. 169.
- Chieng, C. C. and B. E. Launder, 1980. On the calculation of turbulent heat transport downstream from an abrupt pipe expansion, Numerical Heat Transfer, 3, p. 189.
- Eckert, E. R. G., E. M. Sparrow, R. J. Goldstein, C. J. Scott, W. E. Ibele and E. Pfender, 1971. Heat transfer - A review of 1970 literature, Int. J. Heat Mass Transfer, 14, p. 1883.
- Ede, A. J., C. E. Hislop and R. Morris, 1956. Effect on the local heat transfer coefficients in a pipe of an abrupt disturbance of the fluid flow: Abrupt convergence and divergence of diameter ratio 2/1, Proc. Inst. Mech. Eng., London, 170, p. 1113.
- Fletcher, L. S., D. G. Briggs and R. H. Page, 1974. Heat transfer in separated and reattached flows: an annotated review, Israel Journal of Technology, 12, p. 236.
- Gosman, A. D. and W. M. Pun, 1974. Lecture notes for course entitled "Calculation of recirculating flows," Imperial College, Mech. Eng. Dept. Report HTS/74/2.
- Habib, M. A., 1980. Confined flows with and without swirl, Ph.D. Thesis, Imperial College, London.
- Habib, M. A. and J. H. Whitelaw, 1980. Velocity characteristics of a confined coaxial jet with and without swirl, ASME J. Fluids Engng., 102, p. 47.
- Habib, M. A. and J. H. Whitelaw, 1981. Calculations of confined coaxial-jet flows, Third Symposium on Turbulent Shear Flows, University of Calif., Davis, Sept. 9-11, 1981.
- Kays, W. M., 1966. Convective Heat and Mass Transfer, New York: McGraw-Hill.

- Khalil, E. E. and J. H. Whitelaw, 1974. The calculation of local-flow properties in two-dimensional furnaces, Imperial College, Mech. Eng. Dept. Rpt. HTS/74/38.
- Kline, S. J. and F. A. McClintock, 1953. Describing uncertainties in single-sample experiments, Mech. Eng., 75, pp. 3-8.
- Krall, K. M. and E. M. Sparrow, 1966. Turbulent heat transfer in the separated, reattached and redevelopment regions of a circular tube, ASME J. Heat Transfer, 88, p. 131.
- Launder, B. E. and D. B. Spalding, 1974. The numerical computations of turbulent flows, Computer Methods in Applied Mechanics, 3, p. 269.
- McEligot, D. M., P. M. Magee and G. Leppert, 1965. Effect of large temperature gradients on convective heat transfer: the downstream region, J. Heat Transfer, 87, pp. 67-76.
- Morse, A. 1980. Axisymmetric turbulent shear flows with and without swirl, Ph.D. Thesis, University of London, England.
- Patankar, S. V. and D. B. Spalding, 1972. A calculation procedure for heat, mass and momentum transfer in three-dimensional parabolic flows, Int. J. Heat Mass Transfer, 15, p. 1787.
- Pope, S. B. and J. H. Whitelaw, 1976. The calculation of near-wake flows, J. Fluid Mech., 73, p. 9.
- Rodi, W., 1979. Influence of buoyancy and rotation on equations for the turbulent length scale, 2nd Symposium on Turbulent Shear Flows, July 2-4, Imperial College, London.
- Spalding, D. B., 1967. Heat transfer from turbulent separated flows, J. Fluid Mech., 27, p. 97.
- Zaherdadeh, N. H. and B. S. Jagdish, 1975. Heat transfer in decaying swirl flow, Int. J. Heat Mass Transfer, 18, p. 941.
- Zemanick, P. P. and R. S. Dougall, 1970. Local heat transfer downstream of abrupt circular channel expansion, ASME J. Heat Transfer, 92, p. 53.

DISTRIBUTION LIST

HEAT TRANSFER

One copy except
as noted

Mr. M. Keith Ellingsworth
Materials and Mechanics Programs
Office of Naval Research
800 N. Quincy Street
Arlington, VA 22203

5

Defense Documentation Center
Building 5, Cameron Station
Alexandria, VA 22314

12

Technical Information Division
Naval Research Laboratory
4555 Overlook Avenue SW
Washington, DC 20375

6

Professor Paul Marto
Department of Mechanical Engineering
US Naval Post Graduate School
Monterey, CA 93940

Professor Bruce Rankin
Naval Systems Engineering
US Naval Academy
Annapolis, MD 21402

Office of Naval Research Eastern/
Central Regional Office
Bldg 114, Section D
666 Summer Street
Boston, Massachusetts 02210

Office of Naval Research Branch Office
536 South Clark Street
Chicago, Ill. 60605

Office of Naval Research
Western Regional Office
1030 East Green Street
Pasadena, CA 91106

Mr. Charles Miller, Code 05R13
Crystal Plaza #6
Naval Sea Systems Command
Washington DC 20362

Steam Generators Branch, Code 5222
National Center #4
Naval Sea Systems Command
Washington, DC 20362

Heat Exchanger Branch, Code 5223
National Center #3
Naval Sea Systems Command
Washington, DC 20362

Mr. Ed Ruggiero, NAVSEA 08
National Center #2
Washington, DC 20362

Dr. Earl Quandt Jr., Code 272
David Taylor Ship R&D Center
Annapolis, MD 21402

Mr. Wayne Adamson, Code 2722
David Taylor Ship R&D Center
Annapolis, MD 21402

Dr. Win Aung
Heat Transfer Program
National Science Foundation
Washington, DC 20550

Mr. Michael Perlsweig
Department of Energy
Mail Station E-178
Washington, DC 20545

Dr. W.H. Thielbahr
Chief, Energy Conservation Branch
Dept. of Energy, Idaho Operations Office
550 Second Street
Idaho Falls, Idaho 83401

Professor Ephriam M. Sparrow
Department of Mechanical Engineering
University of Minnesota
Minneapolis, Minnesota 55455

Professor J.A.C. Humphrey
Department of Mechanical Engineering
University of California, Berkeley
Berkeley, California 94720

Professor Brian Launder
Thermodynamics and Fluid Mechanics Division
University of Manchester
Institute of Science & Technology
P088 Sackville Street
Manchester M601QD England

Professor Shi-Chune Yao
Department of Mechanical Engineering
Carnegie-Mellon University
Pittsburgh, PA 15213

Professor Charles B. Watkins
Chairman, Mechanical Engineering Department
Howard University
Washington, DC 20059

Professor Adrian Bejan
Department of Mechanical Engineering
University of Colorado
Boulder, Colorado 80309

Professor Donald M. McEligot
Department of Aerospace and Mechanical Engineering
Engineering Experiment Station
University of Arizona 85721

Professor Paul A. Libby
Department of Applied Mechanics and Engineering Sciences
University of California San Diego
Post Office Box 109
La Jolla, CA 92037

Professor C. Forbes Dewey Jr.
Fluid Mechanics Laboratory
Massachusetts Institute of Technology
Cambridge, Massachusetts 02139

Professor William G. Characklis
Dept. of Civil Engineering and Engineering Mechanics
Montana State University
Bozeman, Montana 59717

Professor Ralph Webb
Department of Mechanical Engineering
Pennsylvania State University
208 Mechanical Engineering Bldg.
University Park, PA 16802

Professor Warren Rohsenow
Mechanical Engineering Department
Massachusetts Institute of Technology
77 Massachusetts Avenue
Cambridge, Massachusetts 02139

Professor A. Louis London
Mechanical Engineering Department
Bldg. 500, Room 5018
Stanford University
Stanford, CA 94305

Professor James G. Knudsen
Associate Dean, School of Engineering
Oregon State University
219 Covell Hall
Corvallis, Oregon 97331

Professor Arthur E. Bergles
Mechanical Engineering Department
Iowa State University
Ames, Iowa 50011

Professor Kenneth J. Bell
School of Chemical Engineering
Oklahoma State University
Stillwater, Oklahoma 74074

Dr. James Lorenz
Component Technology Division
Argonne National Laboratory
9700 South Cass Avenue
Argonne, Illinois 60439

Dr. David M. Eissenberg
Oak Ridge National Laboratory
P.O. Box Y, Bldg. 9204-1, MS-0
Oak Ridge, Tennessee 37830

Dr. Jerry Taborek
Technical Director
Heat Transfer Research Institute
1000 South Fremont Avenue
Alhambra, CA 91802

Dr. Simion Kuo
Chief, Energy Systems
Energy Research Laboratory
United Technology Research Center
East Hartford, Connecticut 06108

Mr. Jack Yampolsky
General Atomic Company
P.O. Box 81608
San Diego, CA 92138

Mr. Ted Carnavos
Noranda Metal Industries, Inc.
Prospect Drive
Newtown, Connecticut 06470

Dr. Ramesh K. Shah
Harrison Radiator Division
General Motors Corporation
Lockport, New York 14094

Dr. Ravi K. Sakhuja
Manager, Advanced Programs
Thermo Electron Corporation
101 First Avenue
Waltham, Massachusetts 02154

Mr. Robert W. Perkins
Turbotec Products, Inc.
533 Downey Drive
New Britain, Connecticut 06051

Dr. Keith E. Starnes
York Division, Borg-Warner Corp.
P.O. Box 1592
York, PA 17405

Mr. Peter Wishart
C-E Power Systems
Combustion Engineering, Inc.
Windsor, Connecticut 06095

Mr. Henry W. Braum
Manager, Condenser Engineering Department
Delaval
Front Street
Florence, New Jersey 08518

Dr. Thomas Rabas
Steam Turbine-Generator Technical Operations Division
Westinghouse Electric Corporation
Lester Branch
P.O. Box 9175 N2
Philadelphia, PA 19113

Dr. Al Wood
Director, Mechanics Program
Office of Naval Research
800 N. Quincy Street
Arlington, VA 22203

Mr. Walter Ritz
Code 033C
Naval Ships Systems Engineering Station
Philadelphia, Pa 19112

Mr. Richard F. Wyvill
Code 5232
NC #4
Naval Sea Systems Command
Washington, DC 20362

Mr. Doug Marron
Code 5231
NC #4
Naval Sea Systems Command
Washington, DC 20362

Mr. T. M. Herder
Bldg. 46462
General Electric Co.
1100 Western Avenue
Lynn, MA 01910

Mr. Ed Strain
AiResearch of Arizona
Dept. 76, Mail Stop 301-2
P. O. Box 5217
Phoenix, AZ 85010
(Tel. 602-267-2797)

Mr. Norm McIntire
Solar Turbines International
2200 Pacific Highway
San Diego, CA 92101

Prof. Daryl Metzger
Chairman, Mechanical and Energy
Systems Engineering
Arizona State University
Tempe, AZ 85281

